



**HAL**  
open science

# A Sufficient Condition for the Absence of Two-Dimensional Instabilities of an Elastic Plate in a Duct with Compressible Flow

Jean-François Mercier

► **To cite this version:**

Jean-François Mercier. A Sufficient Condition for the Absence of Two-Dimensional Instabilities of an Elastic Plate in a Duct with Compressible Flow. *SIAM Journal on Applied Mathematics*, 2018, 78 (6), pp.3119-3144. 10.1137/18M1165761 . hal-02381057

**HAL Id: hal-02381057**

**<https://inria.hal.science/hal-02381057v1>**

Submitted on 26 Nov 2019

**HAL** is a multi-disciplinary open access archive for the deposit and dissemination of scientific research documents, whether they are published or not. The documents may come from teaching and research institutions in France or abroad, or from public or private research centers.

L'archive ouverte pluridisciplinaire **HAL**, est destinée au dépôt et à la diffusion de documents scientifiques de niveau recherche, publiés ou non, émanant des établissements d'enseignement et de recherche français ou étrangers, des laboratoires publics ou privés.

1                    **A SUFFICIENT CONDITION FOR THE ABSENCE OF 2D**  
2                    **INSTABILITIES OF AN ELASTIC PLATE IN A DUCT WITH**  
3                    **COMPRESSIBLE FLOW\***

4                    J-F. MERCIER<sup>†</sup>

5                    **Abstract.** We study the time-harmonic resonance of a finite-length elastic plate in a fluid in  
6 uniform flow confined in a duct. Although the resonance frequencies are usually real, the combined  
7 effects of plate elasticity and of a flow can create complex frequencies, different from the usual so-  
8 called scattering frequencies, corresponding to instabilities. We study theoretically the existence of  
9 instabilities versus several problem parameters, notably the flow velocity and the ratio of densities  
10 and of sound speeds between the plate and the fluid. A 3D-volume in the parameters space is defined,  
11 in which no instability can develop. In particular it corresponds to a low enough velocity or a light  
12 enough plate. The theoretical estimates are validated numerically.

13                    **1. Introduction.** We are interested in an acoustic fluid-structure problem: an  
14 elastic finite plate surrounded by a compressible uniform flow confined in a rigid  
15 waveguide. We consider the time harmonic regime: all the quantities vary like  $e^{-i\omega t}$   
16 where  $\omega$  is the frequency.

17                    In this paper we focus on the resonance frequencies: the frequencies for which  
18 there is non-uniqueness in the associated scattering problem, with a solution of the  
19 homogeneous problem in the  $L^2$ -space. It means that without any acoustic source,  
20 fluid vibrations and plate deformations, periodic in time and with finite energy, can  
21 exist. This solution is called a trapped mode since it is confined to the vicinity of  
22 the obstacle and do not radiate energy. Therefore, these trapped modes are of great  
23 physical importance because at the resonance frequencies, the response to a forced  
24 excitation can be quite high.

25                    The case of real resonance frequencies ( $\Im m(\omega) = 0$ ) has already been studied  
26 [1, 2]. These frequencies are obtained as eigenvalues of a self-adjoint operator. Due to  
27 the fluid-structure coupling, a quadratic eigenvalue problem is involved, in which the  
28 resonance frequencies  $\omega$  solve the equations  $\lambda(\omega) = \omega^2$  where  $\lambda$  are the eigenvalues  
29 of an operator of the form  $A + \omega B$ . Then the method is in two steps. For a fixed  
30  $\omega$  value, the spectrum of the operator is made of a continuous essential spectrum  
31 and of eigenvalues below the essential spectrum ( $\omega < \omega_c$  defined in Eq. (6)). We  
32 restricted to the discrete spectrum which is studied thanks to the Min-Max principle.  
33 In particular we proved the existence of eigenvalues  $\lambda_i(\omega)$ ,  $i = 1, \dots, N$  and we  
34 determined theoretical lower bounds for  $N$ . Then the fixed-point equations  $\lambda_i(\omega) =$   
35  $\omega^2$ ,  $i = 1, \dots, N$  are solved. The number of resonances has been estimated versus  
36 various parameters, notably the flow velocity and the rigidity of the plate.

37                    This study of real resonances has revealed an interesting behavior: when the fluid-  
38 structure problem is decoupled (rigid plate or fluid at rest), the resonance frequencies  
39 are necessarily real [1] (see also lemma 7). But when both effects are present, fluid  
40 in flow and elastic plate, the resonance frequencies can be complex [2]. This is the  
41 object of this paper, to study theoretically the resonance frequencies with  $\Im m(\omega) > 0$ .  
42 These complex frequencies are particularly interesting because they correspond to a  
43 stronger transient response to a source of frequency  $\omega$  than for real frequencies: for  
44 a real resonance, the response varies like  $te^{-i\omega t}$  whereas the response grows expo-

---

\*

<sup>†</sup>POEMS, CNRS-INRIA-ENSTA UMR 7231, 828 Boulevard des Maréchaux, 91762 Palaiseau, France ([jean-francois.mercier@ensta-paristech.fr](mailto:jean-francois.mercier@ensta-paristech.fr)).

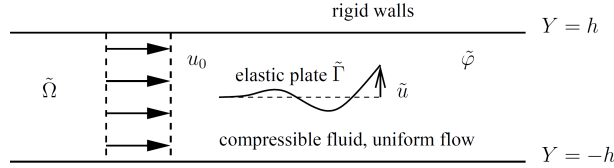
45 nentially for a complex resonance, like  $e^{\Im m(\omega)t}$ . This latter case corresponds to the  
 46 flutter instability encountered in aeroelasticity of airfoils [3, 4]. More generally the  
 47 interaction of a finite flexible panel with a fluid flow with which the plate is aligned  
 48 is a fundamental problem that has received a large attention because of its practical  
 49 importance [5]. The main application lies in aerospace with the study of the airfoil  
 50 flutter of a flexible plate immersed in an axial flow. This instability is similar to flag  
 51 flutter and results from the competition between fluid forces and elasticity. The flutter  
 52 instability has also applications in paper industry or snoring. Experimental [6] and  
 53 numerical [7] studies have been carried out to clarify the paper flutter phenomenon,  
 54 which currently limits the speed of printing machines and paper machines. Besides  
 55 to study human snoring, the stability of a flexible cantilevered plate in channel flow  
 56 has been studied as a representation of the dynamics of the human upper airway  
 57 [8]. The focus is on instability mechanisms of the flexible plate that cause airway  
 58 blockage during sleep. A last class of applications concerns nuclear engineering where  
 59 parallel-plate assemblies are used as core elements in some nuclear research and power  
 60 reactors. References on these subjects may be found in [9].

61 To our knowledge, this study is new. Most of the works on trapped modes concern  
 62 a rigid body and a compressible fluid at rest [10, 11, 12], the main application being  
 63 the water-waves trapped by vertical cylinders of various cross-section shapes. Unlike  
 64 the case of an unbounded flexible wall [13], works on a bounded elastic body and a  
 65 fluid in flow are rather focused on an incompressible flow [14] or a slightly compressible  
 66 flow [15, 16, 17, 18]. Some studies consider the case of a compressible flow, but mostly  
 67 for a membrane structure, not an elastic body, with applications to the control of noise  
 68 [19, 20, 21]. The case of an elastic structure in a compressible flow has been treated but  
 69 in conditions different from ours [22]: although we consider a rectangular geometry in  
 70 the time-harmonic regime with an elastic plate clamped-free, in [22] is considered a  
 71 cylindrical geometry in the time-domain with clamped-clamped boundary conditions.  
 72 The configuration in [22] is a flow in a cylindrical tube, a portion of which is flexible:  
 73 it is mostly a membrane and some results are given for a shell structure. Although  
 74 these differences, a critical velocity  $U_c$  is defined in [22] to which we will compare (see  
 75 paragraph 5.3). The critical velocity is derived using an alternative approach to ours,  
 76 which consists in determining that a positive energy can be defined for  $U < U_c$ .

77 The outline of this paper is as follows. In the second section is presented the  
 78 problem and the definition of what we call an instability is given. In the third section  
 79 is derived a general criterion for the existence of instabilities and this criterion is  
 80 precised in section 4: it is written in terms of the problem parameters, the ratio of  
 81 densities  $\mu$ , the flow velocity  $U$  and the ratio of sound speeds  $c$ . In particular, a volume  
 82 in the space  $(\mu, U, c)$  is defined such that no instabilities can develop in this volume.  
 83 In section 5, the boundaries of this volume are further investigated. In particular,  
 84 thanks to an approximation, threshold values  $\mu_c$  and  $U_c$  are explicitly derived such  
 85 that instabilities can develop only above these thresholds:  $\mu > \mu_c$  and  $U > U_c$ .  
 86 Finally, numerical validations of the derived theoretical estimates are presented in  
 87 section 6.

## 88 2. The general framework.

89 **2.1. Geometry and dimensional equations.** The geometry is shown in Fig.  
 90 1: we consider the 2D waveguide  $\tilde{\Omega} = \{(X, Y) \in \mathbb{R} \times ]-h, h[ \}$  filled with a compressible  
 91 fluid. In the centre of the guide is placed an elastic plate  $\tilde{\Gamma} = \{(X, Y), X \in ]0, L[, Y =$   
 92  $0\}$ . The fluid is in flow with a uniform velocity  $u_0 \mathbf{e}_X$ . We take  $0 < u_0 < c_0$  (subsonic  
 93 flow) where  $c_0$  is the uniform fluid sound speed.


FIG. 1. *Geometry of the problem*

94 In time-harmonic regime of frequency  $\tilde{\omega}$ , if we send an incident wave  $e^{i\tilde{\omega}(X/c_0-t)}$   
95 from  $X = -\infty$  on the plate and if we look for the scattered field, the problem is  
96 found well-posed except for a sequence of so-called resonance frequencies [1, 2]. These  
97 resonances correspond to the existence of eigenmodes (called also trapped modes):  
98 solutions in  $L^2(\tilde{\Omega})$  of the problem without source. In this paper we focus on these  
99 trapped modes and therefore we look for a solution of the following homogeneous  
100 problem [1, 2]:

$$(1) \quad \left\{ \begin{array}{l} \left( \frac{\partial^2}{\partial X^2} + \frac{\partial^2}{\partial Y^2} \right) \tilde{\varphi} = \left( \frac{\tilde{D}}{c_0} \right)^2 \tilde{\varphi} \quad \text{in } \tilde{\Omega} \setminus \tilde{\Gamma}, \\ \left( B \frac{d^4}{dX^4} - \rho_p h_p \tilde{\omega}^2 \right) \tilde{u} = -[p](X, 0) \quad \text{on } \tilde{\Gamma}, \\ p(X, Y) = -\rho_a \tilde{D} \tilde{\varphi}(X, Y) \quad \text{in } \tilde{\Omega} \setminus \tilde{\Gamma}, \\ \frac{\partial \tilde{\varphi}}{\partial Y}(X, 0^\pm) = \tilde{D} \tilde{u} \quad \text{on } \tilde{\Gamma}, \\ \frac{\partial \tilde{\varphi}}{\partial Y}(X, \pm h) = 0 \quad \text{for } X \in \mathbb{R}, \\ \tilde{u}(0) = 0 = \tilde{u}'(0), \quad \tilde{u}''(L) = 0 = \tilde{u}'''(L), \end{array} \right.$$

102 where  $p$  is the fluid pressure,  $\tilde{\varphi}$  the fluid velocity potential and  $\tilde{u}$  the vertical displace-  
103 ment of the plate. The velocity potential satisfies the convected Helmholtz equation  
104 whereas the displacement is solution of the linear plate equation. We have introduced  
105  $[p](X, 0) = p(X, 0^+) - p(X, 0^-)$  the pressure jump through the plate and

$$106 \quad \tilde{D} = u_0 \frac{\partial}{\partial X} - i\tilde{\omega},$$

107 the convective operator. The densities are  $\rho_a$  for the fluid (typically the air) and  $\rho_p$   
108 for the plate. The plate of width  $h_p$  (supposed very small, the plate is seen as 1D)  
109 and of flexural rigidity  $B$ , is clamped at its leading edge  $X = 0$  and free at its trailing  
110 edge  $X = L$ .

111 **2.2. Some symmetries considerations.** In the following we will restrict to an  
112 antisymmetric problem. Indeed, if the obstacle is symmetric and positioned symmetrically  
113 about the waveguide centerline, the solution can be decomposed into a symmetric  
114 and an antisymmetric part about that line. Antisymmetric trapped modes are gener-  
115 ally looked for because the continuous spectrum of the antisymmetric solution has  
116 a nonzero lower limit given by the first duct cut-off frequency (see paragraph 2.4.4).  
117 Then the corresponding antisymmetric trapped modes can be found as discrete eigen-  
118 values below the first cut-off frequency. On the contrary, for symmetric modes, all  
119 the spectrum is continuous.

120 Trapped modes can be determined if the obstacle is no longer symmetric about  
121 the waveguide centerline but this situation is mathematically more complicated. In

122 this case, possible discrete trapped mode frequencies are embedded in the continuous  
 123 spectrum of the relevant operator, and one speaks of embedded trapped modes [23,  
 124 24, 25].

125 Since we only study antisymmetric modes, we can restrict to a half guide:  $Y \in$   
 126  $]0, h[$ , the boundary condition  $[p](X, 0)$  becomes  $2p(X, 0)$  and the boundary condition  
 127  $\tilde{\varphi}(X, 0) = 0$  for  $X \notin [0, L]$  has to be added.

128 **2.3. Dimensionless equations and reduction to a half guide.** Following  
 129 [9], we introduce the parameter  $\gamma$  such that

$$130 \quad \gamma^2 = \frac{B}{\rho_p h_p},$$

131 and the following dimensionless parameters:

$$132 \quad \alpha = \frac{h}{L}, \quad \mu = \frac{\rho_a L}{\rho_p h_p}, \quad c = c_0 \frac{L}{\gamma}.$$

133  $\alpha$  is an aspect ratio,  $\mu$  compares the fluid and plate densities and  $c$  can be seen  
 134 as the ratio of the fluid and plate sound speed. Following [9] we also introduce the  
 135 dimensionless variables  $x = X/L$ ,  $y = Y/h$  and the following dimensionless quantities:  
 136 velocity  $U$ , velocity potential  $\varphi$ , vertical plate displacement  $u$  and frequency  $\omega$  defined  
 137 by

$$138 \quad u_0 = \frac{\gamma}{L} U, \quad \tilde{\varphi} = \gamma \varphi, \quad \tilde{u} = Lu, \quad \tilde{\omega} = \frac{\gamma}{L^2} \omega.$$

139 We note  $\Omega = \{(x, y) \in \mathbb{R} \times ]0, 1[ \}$  the half wave guide,  $\Gamma = \{(x, y), x \in ]0, 1[, y = 0 \}$   
 140 the plate and  $\Sigma = \{(x, y), x \in \mathbb{R}, y = 1 \}$  the upper wall. Also we introduce  $\Gamma^- =$   
 141  $\{(x, y), x < 0, y = 0 \}$  and  $\Gamma^+ = \{(x, y), x > 1, y = 0 \}$  (see Fig. 2) such that  $\Gamma^- \cup \Gamma \cup \Gamma^+$   
 142 is the lower wall of the half-guide.

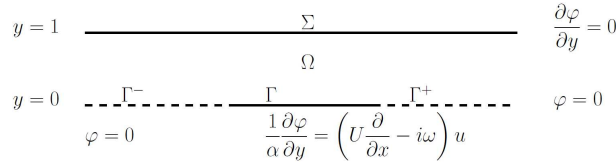


FIG. 2. Geometry restricted to the half-guide

143 Finally, the problem (1) written in a half waveguide in dimensionless form is

$$144 \quad (2) \quad \left\{ \begin{array}{l} \left( \frac{\partial^2}{\partial x^2} + \frac{1}{\alpha^2} \frac{\partial^2}{\partial y^2} \right) \varphi = \frac{1}{c^2} \left( U \frac{\partial}{\partial x} - i\omega \right)^2 \varphi \quad \text{in } \Omega, \\ \left( \frac{d^4}{dx^4} - \omega^2 \right) u = 2\mu \left( U \frac{\partial}{\partial x} - i\omega \right) \varphi(x, 0) \quad \text{on } \Gamma, \\ \frac{1}{\alpha} \frac{\partial \varphi}{\partial y}(x, 0) = \left( U \frac{\partial}{\partial x} - i\omega \right) u \quad \text{on } \Gamma, \\ \frac{\partial \varphi}{\partial y}(x, 1) = 0 \quad \text{on } \Sigma, \\ \varphi(x, 0) = 0 \quad \text{on } \Gamma^\pm, \\ u(0) = 0 = u'(0) \quad \text{and} \quad u''(1) = 0 = u'''(1). \end{array} \right.$$

145 This is a non-linear eigenvalue problem in which  $\omega$  is the eigenvalue. As we will see,  
 146 these eigenvalues can be divided in real and complex eigenvalues.

147 **2.4. Some generalities on the trapped modes.**

148 **2.4.1. Definition of a resonance frequency.** We are interested in the exist-  
149 tence, for a complex frequency, of an acoustic field trapped around the plate, that we  
150 call a resonance:

151 **DEFINITION 1.** *We say that*  
152  $\omega \in \mathbb{C}$  *is a resonance frequency*  $\Leftrightarrow \exists(\varphi, u) \in L^2(\Omega) \times L^2(\Gamma)$  *solution of (2).*  
153  $(\varphi, u)$  *is called the associated trapped mode.*

154 In practice it is more convenient to express the eigenproblem in a variational form.  
155 Thanks to the introduction of the functional spaces

156 (3) 
$$V = \{\varphi \in H^1(\Omega), \varphi = 0 \text{ on } \Gamma^\pm\},$$

157 and

158 (4) 
$$W = \{u \in H^2(\Gamma), u(0) = 0 = u'(0)\},$$

159 and of the sequilinear form on  $V \times W$ :

160 
$$b[(\varphi, u), (\psi, v)] = \int_{\Omega} (1 - M^2) \frac{\partial \varphi}{\partial x} \frac{\partial \bar{\psi}}{\partial x} + \frac{1}{\alpha^2} \frac{\partial \varphi}{\partial y} \frac{\partial \bar{\psi}}{\partial y} - i \frac{\omega}{c} M \left( \frac{\partial \varphi}{\partial x} \bar{\psi} - \varphi \frac{\partial \bar{\psi}}{\partial x} \right) + \frac{1}{2\mu\alpha} \int_{\Gamma} \frac{d^2 u}{dx^2} \frac{d^2 \bar{v}}{dx^2},$$
  
161 
$$+ \frac{1}{\alpha} \int_{\Gamma} \bar{\psi} \left( U \frac{\partial u}{\partial x} - i\omega u \right) + \varphi \left( U \frac{\partial \bar{v}}{\partial x} + i\omega \bar{v} \right) - \omega^2 \left( \frac{1}{c^2} \int_{\Omega} \varphi \bar{\psi} + \frac{1}{2\mu\alpha} \int_{\Gamma} u \bar{v} \right),$$

162 where we have introduced the Mach number  $M \equiv U/c$ , we can write the following  
163 equivalent variational formulation of the eigenvalue problem (2):

164 **DEFINITION 2.**  $\omega \in \mathbb{C}$  *is a resonance frequency*  $\Leftrightarrow \exists(\varphi, u) \in V \times W$  *such that*  
165  $\forall(\psi, v) \in V \times W, b[(\varphi, u), (\psi, v)] = 0.$

166 We have three remarks:

- 167 • The space  $V$  plays the role of radiation conditions. Indeed away from the plate  
168 the velocity potential is decomposed on the duct modes, see Eq. (27) and  
169 more generally see Appendix A for the definition of the duct modes. Since the  
170 propagating modes are not in  $H^1(\Omega)$ , only the decreasing evanescent modes  
171 are selected when restricting to solutions in  $V$ , which leads to a solution  
172 trapped around the plate. In complement to the definition 2 corresponding  
173 to an unbounded domain, in Appendix A are defined the radiation conditions  
174 at finite distance which enables us to define in Appendix B the resonance  
175 problem set in a bounded domain. The equivalence between the two problems  
176 is also proved.
- 177 • The integration by parts leading to  $b[(\varphi, u), (\psi, v)]$  involves the boundary term

178 
$$- \left[ \frac{U}{\alpha} \varphi \bar{v} \right] (1, 0).$$

179 We have imposed a Kutta condition at the trailing edge of the plate: we have  
180 set this term to zero by assuming that the condition  $\varphi(x > 1, 0) = 0$   
181 can be extended by continuity to  $x = 1$ . Another classical Kutta condition is to  
182 impose the fluid velocity to be finite at the plate trailing edge. This requires  
183 to use sophisticated tools like a Wiener-Hopf approach [26, 27] and makes  
184 our analysis method inapplicable. The choice of the right Kutta condition is

important since such choice has been proved to have strong influence on the far-field, in particular on the upstream radiation pattern [26]. But it seems to have a reduced influence on the unstable frequencies we are studying. Indeed we have compared our results to the results in [27], in which only a rigid plate in a flow is considered. We have found for different flow velocities that when changing the Kutta condition from ours to the finite velocity one, the resonance frequencies are just slightly moved in the complex plane. Even though only the case of a rigid plate and a particular  $\alpha$  value have been tested, we assume that it is a general behavior: when changing of Kutta condition, the resonance frequencies only slightly move in the complex plane.

- written back with dimensional quantities,  $M = u_0/c_0$  and thus  $M < 1$  since the flow is supposed subsonic.

**2.4.2. Properties of the resonance frequencies.** The search of  $\omega$  in the complex plane can be restricted to a fourth of the complex plane since the spectrum of resonance frequencies has some nice properties:

LEMMA 3. *If  $\omega$  is an eigenvalue of (2), then  $-\omega$  and  $\pm\bar{\omega}$  are also eigenvalues.*

*Proof.* By taking the complex conjugated of (2), we deduce immediately that if  $\omega$  is an eigenvalue associated to the eigenmode  $(\varphi, u)$  then so is  $-\bar{\omega}$  simply associated to  $(\bar{\varphi}, \bar{u})$ .

The other property that if  $\omega$  is an eigenvalue then so is  $\bar{\omega}$  is more delicate to obtain. In Appendix B we give the proof for the continuous mathematical problem. The proof is rather technical and requires to restrict the resonance problem to a bounded domain to get compactness properties in order to use the Fredholm alternative.

An alternative proof is given here, easier but restricted to the discretized problem. We have determined numerically the resonance frequencies thanks to a method coupling Finite Elements and a modal expansion. The velocity potential is discretized on a Finite Element basis while the plate displacement is expanded on the modes of the plate (details in Appendix C). This leads to a matrixial problem to solve of the form

$$(5) \quad (A + i\omega B + \omega^2 C)X = 0,$$

where  $A$ ,  $B$  and  $C$  are Finite Element matrices and  $X$  is a vector concatenating the nodal values of  $\varphi$  and the modal components of  $u$ .  $A$ ,  $B$  and  $C$  are real valued matrices with  $A$  and  $C$  symmetric and  $B$  antisymmetric. Then we can prove that if  $\omega$  is an eigenvalue,  $-\omega$  is also an eigenvalue. Indeed  $\omega$  is an eigenvalue is equivalent to  $\det(A + i\omega B + \omega^2 C) = 0$ . Then using that for any matrix  $M$  we have  $\det(M) = \det(M^T)$ , we get that  $\det(A - i\omega B + \omega^2 C) = 0$ . Finally, we have proved that if  $\omega$  is an eigenvalue then  $-\bar{\omega}$  and  $-\omega$  are also eigenvalues. But then, since  $-\omega$  is an eigenvalue,  $\bar{\omega}$  and  $\omega$  are also eigenvalues which ends the proof.  $\square$

**2.4.3. An example of resonances.** To show the complexity of the behaviors of the resonance frequencies versus the various parameters of the problem, we present here a typical example of such behavior. The non-linear eigenvalue problem (5) can be written as a classical (but generalized) eigenvalue problem: noting  $Y = \omega X$ , we get:

$$\begin{pmatrix} 0 & 1 \\ A & iB \end{pmatrix} \begin{pmatrix} X \\ Y \end{pmatrix} = \omega \begin{pmatrix} 1 & 0 \\ 0 & -C \end{pmatrix} \begin{pmatrix} X \\ Y \end{pmatrix}.$$

As proved in the previous paragraph, the search of  $\omega$  in the complex plane can be restricted to a fourth of this plane: we just represent the eigenvalues in the quarter

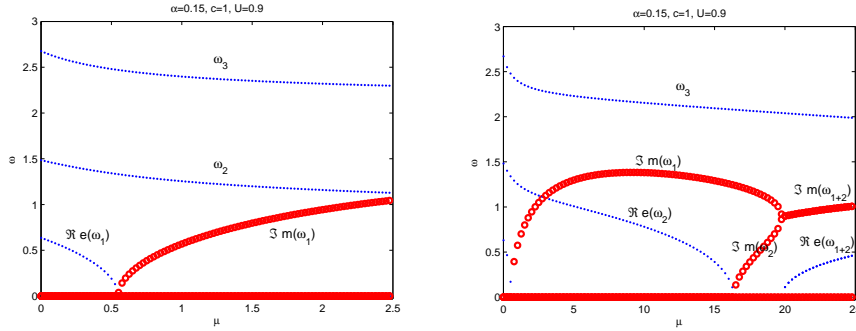


FIG. 3. Three lowest resonance frequencies  $\omega$  when  $\mu$  varies for  $\alpha = 0.15$ ,  $c = 1$  and  $U = 0.9$ .  $\Re e(\omega)$  with dots and  $\Im m(\omega)$  with circles. (a): zoom on the small  $\mu$  values, up to 2.5, (b):  $0 < \mu < 25$

231 plane  $\Re e(\omega) \geq 0$ ,  $\Im m(\omega) \geq 0$ . In Fig. 3 are plotted the evolution of the three lowest  
232 (in the sense  $|\omega|$  small) resonance frequencies when  $\mu$  varies, the other parameters  
233 being fixed:  $c = 1$  and  $U = 0.9$ . In all the figures of this paper, we fix the geometry  
234 and we take  $\alpha = 0.15$  which corresponds to a plate of length  $L \approx 7h$ . The real parts of  
235  $\omega$  are with dots and the imaginary parts are with circles. Fig. 3(b) is for  $0 < \mu < 25$   
236 whereas Fig. 3(a) corresponds to a zoom on the small  $\mu$  values, up to 2.5. We see  
237 in Fig. 3(a) that for small values of  $\mu$  (here  $\mu < \mu_c \equiv 0.55$ ) all the frequencies are  
238 real. At the threshold  $\mu_c$ , the first frequency  $\omega_1$  vanishes and is found to turn from  
239 purely real to purely imaginary. As we will detail latter, it becomes an instability.  
240 In Fig. 3(b), we see that at  $\mu = 16.4$ , the second real frequency  $\omega_2$  becomes purely  
241 imaginary, leading to a second instability for  $\mu > 16.4$ . Moreover, an interesting  
242 event happens at  $\mu = 19.9$ , illustrating the complexity of the resonances behavior and  
243 showing also that the complex frequencies are not necessarily associated to a zero real  
244 part: the two instabilities, purely imaginary, merge to create for  $\mu > 19.9$  a complex  
245 frequency  $\omega_{1+2}$  with non-zero real and imaginary parts. In this paper, we will focus  
246 on the first threshold  $\mu_c$  and we will characterize it: we will derive a lower bound of  
247 this threshold value and also we will find an upper bound of the modulus of the first  
248 unstable frequency (an upper bound of the red curves in Fig. 3).

249 From Fig. 3, it appears that the resonances can be divided in two classes:

250 DEFINITION 4. Let  $\omega \in \mathbb{C}$  be a resonance frequency (definition (2)).

- 251 •  $\Im m(\omega) = 0 \Rightarrow \omega$  is called a real resonance,
- 252 •  $\Im m(\omega) > 0 \Rightarrow \omega$  is called an instability.

253 We will now give some properties of these two kind of resonances.

254 **2.4.4. The real resonance frequencies.** The study of real frequencies has  
255 already been done [1, 2]. They have been looked for below the cut-off frequency  $\omega_c$   
256 of the half wave-guide (with a Dirichlet boundary condition at  $y = 0$ , see Appendix  
257 A)

$$258 \quad (6) \quad \omega < \omega_c \equiv \frac{\pi}{2\alpha} \sqrt{c^2 - U^2}.$$

259 Indeed, only a finite number of eigenfunctions, so-called propagating modes, propagate  
260 undamped along the waveguide while all other so-called evanescent modes decay [28].  
261 Only the propagating modes can radiate energy to infinity and below the cut-off  
262 frequency  $\omega_c$ , all the guided modes are evanescent (see Appendix A). Then the velocity



263 potential  $\varphi$ , which away from the plate can be decomposed on the guided modes,  
 264 naturally decreases exponentially when  $|x| \rightarrow \infty$ : it is localized around the plate and  
 265 thus called a trapped mode.

266 Above the cut-off frequency, some resonance frequencies may exist, but they are  
 267 embedded in the continuous spectrum and their mathematical study is much more  
 268 involved [23, 24, 25].

269 **2.4.5. The instabilities.** We consider causal solutions and thus we focus on  
 270 the asymptotic solutions behavior only when  $t \rightarrow \infty$ . The second case  $\Im m(\omega) > 0$   
 271 corresponds to an unstable behavior since  $e^{-i\omega t} = e^{-i\Re(\omega)t} e^{\Im m(\omega)t}$  and  $e^{\Im m(\omega)t} \rightarrow \infty$   
 272 when  $t \rightarrow \infty$  (we do not restrict when considering that  $\Im m(\omega) > 0$  since if  $\omega$  is a  
 273 resonance frequency,  $\bar{\omega}$  is also a resonance frequency).

274 Note that these unstable frequencies are not the usual “complex resonances” that  
 275 have been studied for rigid bodies [29, 30] or elastic bodies [31, 32]. The complex  
 276 resonances are defined as the poles of the analytical continuation of the resolvent  
 277 scattering operator and are also called scattering frequencies. These poles are very  
 278 different from the unstable frequencies: the associated modes are not trapped but on  
 279 the contrary they grow far from the scattering body. These modes are called leaky  
 280 modes since they have radiation losses. Moreover the analytical continuation is made  
 281 in the half plane  $\Im m(\omega) < 0$  which corresponds to a decreasing behavior in time.  
 282 Therefore the leaky modes cannot correspond to instabilities.

283 To sum up:

- 284 • a complex resonance is bounded in time but not bounded in space,
- 285 • an instability is bounded in space but not bounded in time.

286 In the rest of the paper, to avoid confusion, we will talk about instabilities and not  
 287 complex resonances and we will focus on the existence conditions of these instabilities.

288 **3. General results on the instability frequencies.** First we give general  
 289 properties on the imaginary part of a resonance frequency.

290 **LEMMA 5.** *If  $\omega$  is a resonance frequency and if  $(\varphi, u)$  is the associated trapped*  
 291 *mode, then  $\Im m(\omega)a(\omega; \varphi, u) = 0$  where*

$$292 \quad (7) \quad a(\omega; \varphi, u) = \int_{\Omega} (1 - M^2) \left| \frac{\partial \varphi}{\partial x} \right|^2 + \frac{1}{\alpha^2} \left| \frac{\partial \varphi}{\partial y} \right|^2 + \frac{1}{2\mu\alpha} \int_{\Gamma} \left| \frac{d^2 u}{dx^2} \right|^2$$

$$293 \quad + \frac{2U}{\alpha} \Re \int_{\Gamma} \bar{\varphi} \frac{\partial u}{\partial x} + |\omega|^2 \left( \frac{1}{c^2} \int_{\Omega} |\varphi|^2 + \frac{1}{2\mu\alpha} \int_{\Gamma} |u|^2 \right).$$

294 *Proof.* From definition 2, taking  $(\psi, v) = (\varphi, u)$ , the result is deduced using

$$295 \quad \Im m \left\{ -\frac{1}{\omega} b[(\varphi, u), (\varphi, u)] \right\} = 0. \quad \square$$

296 This lemma has a simple consequence: a general non-existence result for instabil-  
 297 ities, that will be used in all the following of the paper.

298 **LEMMA 6.** *If  $\forall (\varphi, u) \in V \times W$ ,  $a(\omega; \varphi, u) > 0$ , then  $\omega$  cannot be an instability.*

299 *Proof.* This is a consequence of lemma 5 and definition 4:  $\Im m(\omega)a(\omega; \varphi, u) = 0$   
 300 and  $a(\omega; \varphi, u) > 0$  implies  $\Im m(\omega) = 0$ .

301 **REMARK 1.** *In this paper we derive non-existence results for instabilities and we*  
 302 *do not know how to derive an existence result for instabilities. But since in practice*

304 *we wish to avoid instabilities, it is useful to determine in which conditions we are sure*  
 305 *they do not develop.*

306 **REMARK 2.** *We do not discuss if the instabilities we look for are physical (in the*  
 307 *sense causal) solutions. The boundary conditions are assumed to be decay at infinity*  
 308 *for any  $\Im m(\omega)$ , and this is definitely correct for the case we are interested in of*  
 309  *$\Im m(\omega) > 0$ , but may not be physically correct or causal for the other solutions with*  
 310  *$\Im m(\omega) < 0$ , in particular if  $\Im m(\omega)$  is sufficiently negative. This causality question*  
 311 *is complicated when considering complex frequencies but hopefully not essential for us*  
 312 *since we focus on cases for which no instabilities can exist, whether they are causal or*  
 313 *not. If we wanted to describe how to excite an instability, then the causality question*  
 314 *would become essential.*

315 In the rest of the paper, we will derive simple conditions on the parameters of the  
 316 problem under which lemma 6 is fulfilled.

317 **4. Criteria of non-existence of instabilities.** Following lemma 6, for a fixed  
 318 frequency  $\omega$  we look now for conditions, as simple as possible, for which  $a(\omega; \varphi, u) > 0$ ,  
 319  $\forall(\varphi, u) \in V \times W$ .

320 **4.1. A simple criterion.** A first result is, as announced in the introduction,  
 321 that only the joint effects of the elasticity of the plate and of the flow can create  
 322 instabilities:

323 **LEMMA 7.** *If the fluid is at rest ( $U = 0$ ) or the plate rigid ( $u = 0$ ), there is no*  
 324 *instability.*

325 *Proof.* In the expression of  $a(\omega; \varphi, u)$  in (7), all the terms are strictly positive for  
 326  $(\varphi, u) \neq (0, 0)$  excepting the term

$$327 \quad \frac{2U}{\alpha} \Re \int_{\Gamma} \bar{\varphi} \frac{\partial u}{\partial x}. \quad \square$$

328 Therefore, if this term is equal to zero, there is no instability using lemma (6). This  
 329 is the case if  $U = 0$  or  $u = 0$ .

330 As already said, the trapped modes for these uncoupled problems (fluid at rest  
 331 or rigid plate) have already been studied [1]. In this paper we focus on instabilities.

332 **4.2. A general criterion.** We will now state the main theorem of this paper,  
 333 giving an explicit sufficient condition to have no instability. For this theorem, we need  
 334 to introduce some notations. We introduce

$$335 \quad (8) \quad \lambda_1 = \inf_{\varphi \in V \setminus \{0\}} R(\varphi),$$

336 where we have introduced the Rayleigh quotient

$$337 \quad (9) \quad R(\varphi) = \frac{\int_{\Omega} (c^2 - U^2) \left| \frac{\partial \varphi}{\partial x} \right|^2 + \frac{c^2}{\alpha^2} \left| \frac{\partial \varphi}{\partial y} \right|^2}{\int_{\Omega} |\varphi|^2}.$$

338 Also we introduce

$$339 \quad (10) \quad \alpha_1^4 = \inf_{u \in W \setminus \{0\}} \frac{\int_{\Gamma} \left| \frac{d^2 u}{dx^2} \right|^2}{\int_{\Gamma} |u|^2}.$$

340 The values  $\lambda_1$  and  $\alpha_1^4$  are the first eigenvalues of problems that are specified in  
 341 Appendix D. The value  $\lambda_1$  is sometimes called the first eigenvalue of vibration for  
 342 the fluid [22]. Its value is determined numerically and a useful approximation of  $\lambda_1$  is  
 343 derived in Appendix D. In Eq. (10),  $\alpha_1^2 = \omega_1^{\text{plate}}$  where  $\omega_1^{\text{plate}}$  is the first eigenfrequency  
 344 of the plate alone in vacuum. Numerically it is found that  $\alpha_1 = 1.88$ .

345 Finally we introduce

$$346 \quad (11) \quad \hat{\sigma} \equiv \min(\lambda_1, \alpha_1^4),$$

347 and

$$348 \quad (12) \quad \beta = \frac{\alpha}{c} \sqrt{\hat{\sigma}}.$$

349 With these notations, we have the

350 THEOREM 8. *Let*

$$351 \quad (13) \quad T(\omega) \equiv \hat{\sigma} \left[ 1 - U \left( \frac{2}{\beta} + \beta \right) \sqrt{\alpha \mu} \right] + |\omega|^2,$$

352 where  $\hat{\sigma}$  and  $\beta$  are defined in (11) and (12). If  $T(\omega) > 0$ , then  $\omega$  cannot be an  
 353 instability.

354 *Proof.* The idea is to show that  $T(\omega)$  is a lower bound of  $a(\omega; \varphi, u)$  and then to  
 355 use lemma 6. In this aim, first we derive a general lower bound for  $a$ , depending on  
 356 some parameters obtained only numerically. Second, we derive another lower bound,  
 357 a little less accurate, but given in a closed-form and thus easier to utilise.

358 • a general lower bound for  $a(\omega; \varphi, u)$

359 We decompose  $a$  defined in (7) in three parts:  $a = a_1 + a_2 + a_3$ , with

$$360 \quad (14) \quad \begin{cases} a_1(\varphi, u) = \int_{\Omega} (1 - M^2) \left| \frac{\partial \varphi}{\partial x} \right|^2 + \frac{1}{\alpha^2} \left| \frac{\partial \varphi}{\partial y} \right|^2 + \frac{1}{2\mu\alpha} \int_{\Gamma} \left| \frac{d^2 u}{dx^2} \right|^2, \\ a_2(\varphi, u) = \frac{2U}{\alpha} \Re \int_{\Gamma} \bar{\varphi} \frac{\partial u}{\partial x}, \\ a_3(\varphi, u) = |\omega|^2 \|(\varphi, u)\|^2, \end{cases}$$

361 with

$$362 \quad \|(\varphi, u)\|^2 = \frac{1}{c^2} \int_{\Omega} |\varphi|^2 + \frac{1}{2\mu\alpha} \int_{\Gamma} |u|^2.$$

363 We look for a positive lower bound for  $a$  and in this aim, we determine a small  
 364 upper bound for  $|a_2|$ . Using the Poincaré's inequality it is found that  $\forall u \in W$  defined  
 365 in (4)

$$366 \quad (15) \quad \int_{\Gamma} \left| \frac{du}{dx} \right|^2 \leq \frac{1}{2} \int_{\Gamma} \left| \frac{d^2 u}{dx^2} \right|^2.$$

367 We also use the trace inequality:  $\forall \tau > 0$  and  $\forall \varphi \in V$ ,

$$368 \quad (16) \quad \int_{\Gamma} |\varphi|^2 \leq (1 + \tau^2) \int_{\Omega} |\varphi|^2 + \frac{1}{\tau^2} \int_{\Omega} \left| \frac{\partial \varphi}{\partial y} \right|^2.$$

369 This trace inequality is derived by using an alternative of the Poincaré's inequality  
 370 for a fixed value of  $x$ , and then by integrating along the  $x$  axis on the plate  $\Gamma$ .

371 Then, writing  $a_2$  under the form

$$372 \quad a_2 = 2\eta \int_{\Gamma} \frac{\tau}{\alpha} |\varphi| \frac{\left| \frac{du}{dx} \right|}{\sqrt{\mu\alpha}},$$

373 with  $\eta = U\sqrt{\mu\alpha}/\tau$ , we deduce with Young's inequality and then with (15) and (16)  
374 that:

$$375 \quad \frac{|a_2|}{\eta} \leq \int_{\Gamma} \frac{\tau^2}{\alpha^2} |\varphi|^2 + \frac{1}{\mu\alpha} \left| \frac{du}{dx} \right|^2,$$

$$376 \quad \leq \frac{\tau^2(1+\tau^2)}{\alpha^2} \int_{\Omega} |\varphi|^2 + \frac{1}{\alpha^2} \int_{\Omega} \left| \frac{\partial\varphi}{\partial y} \right|^2 + \int_{\Gamma} \frac{1}{2\mu\alpha} \left| \frac{d^2u}{dx^2} \right|^2.$$

377 Then using (14) leads to

$$378 \quad \frac{|a_2|}{\eta} \leq \tau^2(1+\tau^2) \frac{c^2}{\alpha^2} \|(\varphi, u)\|^2 + a_1.$$

379 Finally, using  $a \geq a_1 - |a_2| + a_3$ , we deduce  $\forall(\varphi, u) \in V \times W$ ,  $(\varphi, u) \neq (0, 0)$  and  
380  $\forall\omega \in \mathbb{C}$ :

$$381 \quad \frac{a(\omega; \varphi, u)}{\|(\varphi, u)\|^2} \geq (1-\eta)\sigma^* - \eta\tau^2(1+\tau^2) \frac{c^2}{\alpha^2} + |\omega|^2,$$

382 where

$$383 \quad \sigma^* = \inf_{(\varphi, u) \in V \times W} \frac{a_1(\varphi, u)}{\|(\varphi, u)\|^2}.$$

384 This lower bound is more accurate than  $T$  defined in (13) but requires the use of some  
385 numerics to determine  $\sigma^*$ . To find the closed-form formula (13), we need to evaluate  
386 a more explicit lower bound for  $\sigma^*$ , noted  $\hat{\sigma}$  and also to choose the value of  $\tau$ .

- 387 • an explicit lower bound for  $a(\omega; \varphi, u)$
- 388 ◦ Value of  $\hat{\sigma}$

389 The value of  $\hat{\sigma}$  is obtained by using the inequality for any positive real numbers  
390  $a, b, c$  and  $d$ :

$$391 \quad \frac{a+b}{c+d} \geq \min \left\{ \frac{a}{c}, \frac{b}{d} \right\},$$

392 from which is deduced  $\forall(\varphi, u) \in V \times W$ ,  $(\varphi, u) \neq (0, 0)$

$$393 \quad \frac{a_1(\varphi, u)}{\|(\varphi, u)\|^2} \geq \min \left\{ \frac{\int_{\Omega} (c^2 - U^2) \left| \frac{\partial\varphi}{\partial x} \right|^2 + \frac{c^2}{\alpha^2} \left| \frac{\partial\varphi}{\partial y} \right|^2}{\int_{\Omega} |\varphi|^2}, \frac{\int_{\Gamma} \left| \frac{d^2u}{dx^2} \right|^2}{\int_{\Gamma} |u|^2} \right\},$$

394 which leads to

$$395 \quad \sigma^* \geq \hat{\sigma} \equiv \min(\lambda_1, \alpha_1^4),$$

396 using the definitions (8) and (10). Finally we get

$$397 \quad \frac{a(\omega; \varphi, u)}{\|(\varphi, u)\|^2} \geq T,$$

398 with  $T$  defined by

$$399 \quad T = \hat{\sigma} - \frac{U}{\tau} \sqrt{\mu\alpha} \left[ \hat{\sigma} + \tau^2(1+\tau^2) \frac{c^2}{\alpha^2} \right] + |\omega|^2.$$

400 ◦ Value of  $\tau$

401 To get (13), the value of  $\tau$  has to be chosen. If  $U = 0$ ,  $T(\omega) = \hat{\sigma} + |\omega|^2$  is always  
 402 positive and we recover that all the resonances are real for a fluid at rest (lemma 7).  
 403 For  $U > 0$ , we choose  $\tau$  such that  $T$  remains positive as long as possible when  $U$   
 404 increases. It means that we need

$$405 \quad \frac{\hat{\sigma} + \tau^2(1 + \tau^2)\frac{c^2}{\alpha^2}}{\tau},$$

406 to be small. It is straightforward to check that this quantity is minimum for  $\tau = \hat{\beta}$   
 407 with

$$408 \quad (17) \quad \hat{\beta}^2 = \frac{1}{6} \left( -1 + \sqrt{1 + 12 \frac{\hat{\sigma}\alpha^2}{c^2}} \right). \quad \square$$

409 If  $\hat{\sigma}\alpha^2/c^2$  is large, we get the approximation  $\hat{\beta}^2 \simeq \hat{\sigma}\alpha^2/c^2$ . We have checked numeri-  
 410 cally that  $\hat{\sigma}\alpha^2/c^2$  remains a good approximation of  $\hat{\beta}^2$ , even when it is not large (see  
 411 Fig. 4). Therefore we choose to define  $\tau$  by the value of  $\beta$  in (12) which leads to the  
 412 expression (13) of  $T$ .

413 A nice consequence of Theorem (8) is that we can establish a closed-form criterion  
 414 for the appearance of instabilities. This is done in the next paragraph.

415 **4.3. A threshold for instabilities existence.** Utilizing theorem 8, we can  
 416 deduce a threshold for the possible existence of an instability and also a bounding  
 417 of the modulus of the unstable frequencies above the threshold. If we introduce the  
 418 function

$$419 \quad (18) \quad f(\mu, U, c) = U \left( \frac{2}{\beta} + \beta \right) \sqrt{\alpha\mu},$$

420 we have the

421 **COROLLARY 9.** *A resonance frequency  $\omega$  is necessarily real if*

- 422 •  $f(\mu, U, c) < 1$ ,
- 423 •  $f(\mu, U, c) \geq 1$  and  $|\omega|^2 > \hat{\sigma} [f(\mu, U, c) - 1]$ .

424 *In other words, an instability  $\omega$  can exist only if  $f(\mu, U, c) > 1$  and  $|\omega|^2 \leq$   
 425  $\hat{\sigma} [f(\mu, U, c) - 1]$ .*

426 **REMARK 3.** *When it exists, an instability  $\omega$  is necessarily of small modulus  $|\omega|$   
 427 since  $\omega$  is located in the complex plane ( $\Re(\omega)$ ,  $\Im(\omega)$ ) inside a disc of bounded radius  
 428  $R = \sqrt{\hat{\sigma} [f(\mu, U, c) - 1]}$ .*

429 *Proof.* This corollary is a direct consequence of theorem 8:

$$430 \quad T(\omega) > 0 \Rightarrow \Im(\omega) = 0. \quad \square$$

431 The improvement of corollary 9, compared to theorem 8, is that the conditions leading  
 432 to  $T > 0$  have been written in a closed-form.

433 Although this corollary is rather explicit, it is not so easy to use in practice  
 434 because it describes the joint effects of  $\mu$ ,  $U$  and  $c$ . Before presenting numerical  
 435 validations of the theoretical estimates, in the next section we will simplify corollary  
 436 9 by considering separately the different effects.

437 **5. Analysis of the stability area.** The previous corollary has introduced a  
438 “stability area”, defined by

$$439 \quad (19) \quad f(\mu, U, c) < 1.$$

440 It corresponds to an unbounded volume in the space  $(U, \mu, c)$  in which no instability  
441 can exist and we will now characterize this volume. This volume can be obtained  
442 numerically (see Fig. 7) but we wish here to get closed-form results, easier to utilise.  
443 To do so, an approximation is required: in Appendix D we prove that  $\lambda_1$  defined  
444 in (8) can be approximated by  $\lambda_1 \simeq (c^2 - U^2)\pi^2$ . Thus  $\hat{\sigma}$  defined in (11) can be  
445 approximated by

$$446 \quad (20) \quad \sigma = \min [(c^2 - U^2)\pi^2, \alpha_1^4].$$

447 Since  $\beta$  defined in (12) depends on  $U$  and  $c$ , the dependence of the volume defined  
448 in (19) versus  $U$  or  $c$  is rather involved. On the contrary, the dependence versus  $\mu$   
449 is explicit:  $f$  is an increasing function of  $\mu$  and the relation (19) is obviously not fulfilled  
450 for large  $\mu$  values. For its simplicity, we start by analyzing the dependence versus  $\mu$ .

451 **5.1. Influence of  $\mu$ .**  $\mu$  becomes large when the fluid is heavy and/or the plate  
452 is light and this is necessary for the possible development of instabilities as stated in  
453 the following lemma:

454 LEMMA 10. For  $U$  and  $c$  fixed, an instability  $\omega$  can exist only if

- 455 •  $\mu > \mu_c$ ,
- 456 •  $|\omega|^2 < \hat{\sigma}U \left( \frac{2}{\beta} + \beta \right) \sqrt{\alpha} (\sqrt{\mu} - \sqrt{\mu_c})$ , where the critical threshold  $\mu_c$  is defined

457 by

$$458 \quad (21) \quad \mu_c = g(U, c) \equiv \frac{1}{\alpha U^2 \left( \frac{2}{\beta} + \beta \right)^2}$$

459 *Proof.*  $f$  defined in (18) is obviously an increasing function of  $\mu$ . Therefore, if we  
460 define  $\mu_c$  by  $f(\mu_c, U, c) = 1$  which is equivalent to (21), we deduce that

$$461 \quad \mu < \mu_c \Leftrightarrow f(\mu, U, c) < 1.$$

462 Then the lemma is just a consequence of Corollary (9).  $\square$

463 The validity of this lemma is illustrated in Fig. 4, where are represented the three  
464 first resonance frequencies when  $\mu$  varies for  $\alpha = 0.15$ ,  $c = 1$  and  $U = 0.7$ .  $\Re e(\omega)$   
465 is represented with dots and  $\Im m(\omega)$  with circles. Using (6), the cut-off frequency is  
466  $\omega_c = 7.48$ . Two additional curves represent the function

$$467 \quad (22) \quad h : \begin{cases} \mu \rightarrow 0 & \text{for } \mu < \mu_c, \\ \mu \rightarrow \sqrt{\hat{\sigma}U \left( \frac{2}{\beta} + \beta \right) \sqrt{\alpha} (\sqrt{\mu} - \sqrt{\mu_c})} & \text{for } \mu > \mu_c, \end{cases}$$

468 where  $\mu_c = 0.35$  is determined with (21). The difference between the two curves is the  
469 value of  $\sigma$  and of  $\beta$ : the straight line is an approximated curve evaluated with (20)  
470 and (12) whereas the dashed line is exact and corresponds to the use of (11) and (17).  
471 As announced previously, (20) and (12) are confirmed to be very good approximations  
472 of (11) and (17).

473 Fig. 4 validates Lemma 10: the instability develops for values of  $\mu > 2$ , larger than  
474  $\mu_c$  and the modulus of the unstable frequency (here  $|\Im m(\omega_1)| = |\omega_1|$  since  $\Re e(\omega_1) = 0$   
475 for the instability) is below the solid and dashed curves.

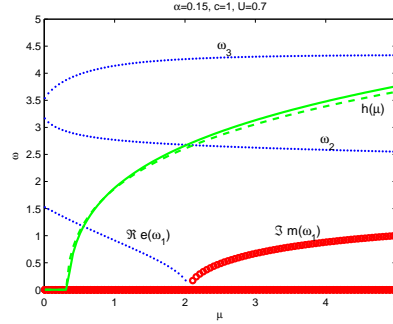


FIG. 4. Three lowest resonance frequencies  $\omega_n$ ,  $n = 1, 2$  and  $3$  when  $\mu$  varies for  $\alpha = 0.15$ ,  $c = 1$  and  $U = 0.7$ .  $\Re(\omega)$  with dots and  $\Im m(\omega)$  with circles. Upper boundary  $h(\mu)$  for  $|\omega|$ , defined in (22): solid line for the approximated boundary and dashed line for the exact one

476 **5.2. Influence of  $U$  and  $c$ .** We study now how varies  $f$  versus  $U$  and  $c$ . To  
 477 simplify the study and get monotonous behaviors, we restrict ourselves to the case  
 478  $\alpha\pi < \sqrt{2}$  which means that the plate is long enough ( $\sqrt{2}L > \pi h$ ).

479 LEMMA 11. For  $\alpha\pi < \sqrt{2}$ ,  $f(\mu, U, c)$  is an increasing function of  $U$  and for values  
 480 of  $c$  such that  $c < \alpha_1^2/\pi$ ,  $f$  is a decreasing function of  $c$ . In other words, an instability  
 481 can occur only for  $U$  large enough or  $c$  small enough.

482 *Proof.* We note  $\theta(x) = \frac{2}{x} + x$  such that  $f$  in (18) is defined by

483 
$$f(\mu, U, c) = U\theta(\beta)\sqrt{\alpha\mu}. \quad \square$$

484 Recalling that there is no instability if  $f(\mu, U, c) < 1$ , we need to evaluate  $\beta$  from (12)  
 485 to conclude. The results depend on the value of  $\sigma = \min[(c^2 - U^2)\pi^2, \alpha_1^4]$  and thus

486 on the sign of  $U^2 + \frac{\alpha_1^4}{\pi^2} - c^2$ :

- 487 • If  $c^2 < U^2 + \frac{\alpha_1^4}{\pi^2}$ , then  $\sigma = (c^2 - U^2)\pi^2$  and thus  $\beta = \alpha\pi\sqrt{1 - M^2}$   
 488 • If  $c^2 > U^2 + \frac{\alpha_1^4}{\pi^2}$ , then  $\sigma = \alpha_1^4$  and thus  $\beta = \frac{\alpha_1^2\alpha}{c} < \alpha\pi\sqrt{1 - M^2}$

489 Therefore, in all cases,  $\beta \leq \alpha\pi$ . Now we use the fact that  $\theta$  is decreasing for  
 490  $x < \sqrt{2}$ . Therefore, if  $\alpha\pi < \sqrt{2}$ ,  $\theta(\beta)$  is a decreasing function of  $\beta$ . The conclusion is  
 491 then easy to deduce:  $f \nearrow$  if

- 492 •  $U \nearrow$ ,  
 493 •  $c^2 < U^2 + \frac{\alpha_1^4}{\pi^2}$  and  $c \searrow$   
 494 •  $c^2 > U^2 + \frac{\alpha_1^4}{\pi^2}$  and  $c \nearrow$ .

495 In particular, if  $c < \alpha_1^2/\pi$ ,  $f \nearrow$  when  $c \searrow$ .

496 To illustrate this lemma, we have represented in Fig. 5 isovalues of the function  
 497  $g(U, c)$  defined in (21). The black thick line is the curve  $c^2 = U^2 + \alpha_1^4/\pi^2$ , which  
 498 corresponds to the change of definition for  $\sigma$  (see (20)). We recall that we have two  
 499 equivalent definitions for the stability area:

500 
$$f(\mu, U, c) < 1 \Leftrightarrow \mu < g(U, c).$$

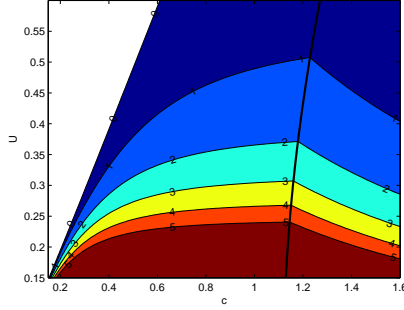


FIG. 5. Isovalues of the function  $g(U, c)$  defined in (21) for  $\alpha = 0.15$ . For  $\mu = \mu_0$ , the area  $g(U, c) > \mu_0$  in the  $(U, c)$  plane is stable. Curve  $c^2 = U^2 + \alpha_1^4/\pi^2$  in black thick line

501 Therefore, if  $\mu = \mu_0$ , the stability zone is defined by the area in the  $(U, c)$  plane such  
502 that  $g(U, c) > \mu_0$ . Values of  $\mu_0$  between 1 and 5 are indicated in Fig. 5. We see that  
503 this area reduces when  $\mu$  increases. We see also that we go out the stability zone  
504 when increasing  $U$  or  $\mu$  or decreasing  $c$  if  $c < \alpha_1^2/\pi$ , in accordance with lemma 11.

505 Contrary to the simple dependence versus  $\mu$ , it is not possible to define, starting  
506 from (19), closed-form critical threshold  $U_c$  and  $c_c$  such that an instability can occur  
507 only for  $U > U_c$  or  $c < c_c$ . However, by approximating (19), it is possible to derive an  
508 approximate value of  $U_c$ , noted  $U_c^{\text{app}}$ , which compares with the one derived in [22].

509 **5.3. Simplifications for the influence of  $U$ .** Still for  $\alpha\pi < \sqrt{2}$ , since  $f(\mu, U, c)$   
510 is an increasing function of  $U$ , we can introduce the threshold frequency  $U_c$  defined  
511 by

$$512 \quad (23) \quad f(\mu, U_c, c) = 1.$$

513 Let us recall that thanks to lemma 11 we have the following alternative:

- 514 • If  $U < U_c \Rightarrow$  no instabilities exist
- 515 • If  $U > U_c \Rightarrow$  instabilities can exist

516 The aim of this paragraph is to look for a closed-form expression of  $U_c$ , as obtained  
517 in [22]. We have

518 LEMMA 12. For  $\alpha\pi < \sqrt{2}$  and  $c < \alpha_1^2/\pi$ ,  $U_c < U_c^{\text{app}}$  where

$$519 \quad (24) \quad (U_c^{\text{app}})^2 = \frac{\alpha\pi^2 c^2}{4\mu c^2 + \alpha\pi^2},$$

520 and  $U_c$  is defined in (23).

521 *Proof.* The condition on  $c$  implies, from (20), that  $\hat{\sigma} = (c^2 - U^2)\pi^2$ . Then we  
522 introduce an approximation of  $f$ , deduced by cancelling the term  $\beta$  in (18). It is thus  
523 defined by

$$524 \quad f^{\text{app}}(\mu, U, c) = U \frac{2}{\beta} \sqrt{\alpha\mu} = \frac{2}{\pi} \sqrt{\frac{\mu U^2 c^2}{\alpha(c^2 - U^2)}}, \quad \square$$

525 and it is such that  $f^{\text{app}} < f$ . To this approximated function is associated an approxi-  
526 mated threshold velocity  $U_c^{\text{app}}$ , defined by  $f^{\text{app}}(\mu, U_c^{\text{app}}, c) = 1$ . It leads to (24) which  
527 is similar to the value in [22] (4 is replaced by 1 in [22], leading to a less precise upper  
528 bound, certainly due to a 1D approximation of the acoustic propagation introduced



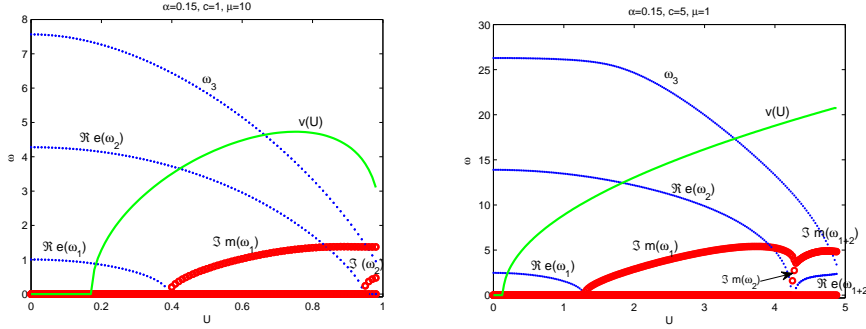


FIG. 6. Three lowest resonance frequencies  $\omega_n$ ,  $n = 1, 2, 3$  when  $U$  varies for  $\alpha = 0.15$ .  $\Re e(\omega)$  with dots and  $\Im m(\omega)$  with circles. Upper boundary  $v(U)$  for  $|\omega|$ , defined in (25), in solid line. (a)  $c = 1$  and  $\mu = 10$ , (b)  $c = 5$  and  $\mu = 1$

529 in [22]). Finally,  $U_c^{\text{app}}$  is less precise than  $U_c$  since it is an upper bound for  $U_c$ : indeed  
 530  $f^{\text{app}} < f$  and  $f^{\text{app}}$  is an increasing function of  $U$ .

531 **6. Numerical validation of the estimates.** The aim of the numerical study  
 532 is mostly to validate corollary 9. First we look the influence of the velocity  $U$ . Then  
 533 we illustrate the validity of the stability area defined in (19).

534 **6.1. Threshold for the velocity.** In Fig. 6 are plotted the three first resonance  
 535 frequencies when  $U$  varies between 0 and  $c$  for  $\alpha = 0.15$  and for two values of  $(c, \mu)$ .  
 536  $\Re e(\omega)$  is represented with dots and  $\Im m(\omega)$  with circles. The green curves represent  
 537 the function

$$538 \quad (25) \quad v : U \rightarrow \sqrt{\max \left\{ 0, \sigma \left[ U \left( \frac{2}{\beta} + \beta \right) \sqrt{\alpha\mu} - 1 \right] \right\}},$$

539 involved in corollary 9 with  $\sigma$  and  $\beta$  evaluated thanks to (20) and (12). Corollary 9  
 540 asserts that an instability  $\omega$  can not exist if  $v(U) = 0$  and that, when it exists, it must  
 541 satisfy

$$542 \quad |\omega| \leq v(U).$$

543 These results are validated since the circles are found below the continuous solid  
 544 curves. Note that in Fig. 6(b), at  $\mu = 4.3$ , two purely imaginary frequencies merge  
 545 to produce a frequency  $\omega_{1+2}$  with non-zero real and imaginary parts for  $\mu > 4.3$  (as  
 546 in Fig. 3(b)). The modulus of the complex frequency  $\omega_{1+2}$  is not represented but it  
 547 is clearly below the values of the green curve.

548 **6.2. Stability area.** Now we focus on the shape of the stability area, defined by  
 549 (19),  $f(\mu, U, c) < 1$ , versus  $\mu$ ,  $U$  and  $c$ . Lemmas 10 and 11 indicate that the stability  
 550 area corresponds to  $\mu$  or  $U$  small enough (the behavior versus  $c$  is more involved). In  
 551 other words, we expect instabilities to appear when increasing  $\mu$  or  $U$ . We will see  
 552 numerically that it is the case and that instabilities only develop outside the stability  
 553 area, confirming the validity of the theoretical estimates. In Fig. 7 are plotted two  
 554 isovalues of the function  $f(\mu, U, c)$  defined in (18) for  $\alpha = 0.15$  and with one parameter  
 555 fixed: Fig. 7 (a) is for  $c = 1$  and Fig. 7 (b) for  $\mu = 1$ . The isovalue  $f(\mu, U, c) = 1$  is  
 556 represented to show the borderline of the theoretical stability area. The isovalue  $f = 2$   
 557 is included to clarify the location of the theoretical stability area  $f(\mu, U, c) < 1$  (it is

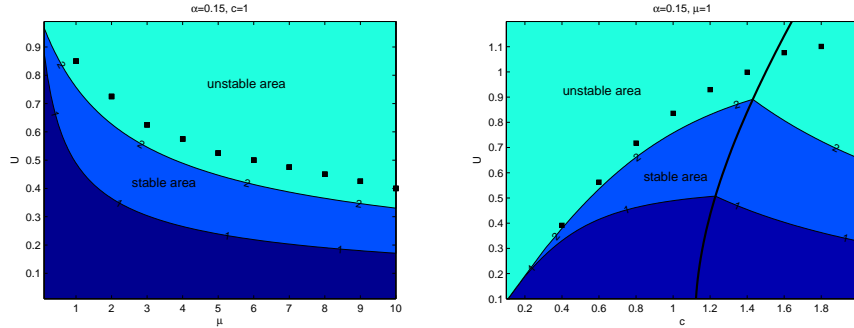


FIG. 7. Isovalues of  $f(\mu, U, c)$  defined in (18) for  $\alpha = 0.15$ . (a)  $c = 1$ , (b)  $\mu = 1$ .

558 enough since  $f$  has monotonous variations). The black squares represent the couple  
559 of values obtained numerically,  $(\mu, U)$  or  $(c, U)$ , for which an instability appears. It  
560 means that the area above the black squares is an unstable area associated with the  
561 effective existence (found numerically) of instabilities. Fig. 7 confirms that the lower  
562 area  $f(\mu, U, c) < 1$  (in dark) corresponds to a stability area since the black squares  
563 are outside this area. Note that the “true” stable area, found numerically, is larger  
564 and in particular it contains the light area located between  $f = 1$  and  $f = 2$ .

565 **7. Conclusion.** We have studied the trapped modes localized around an elastic  
566 plate placed in the center of a rigid waveguide and surrounded by a compressible  
567 fluid in a uniform flow. The case of real resonance frequencies was already known  
568 and we have extended the study to the search of complex frequencies corresponding  
569 to the development of instabilities. We have mainly proved two results: in the space  
570  $(\mu, U, c)$ , there is a “stability” area in which no instability can develop. In particular  
571 it corresponds to  $\mu < \mu_c$  or  $U < U_c$  where  $\mu_c$  and  $U_c$  are threshold values. Moreover,  
572 outside this stability area, if an instability of frequency  $\omega$  develop, necessarily  $\omega$  lies  
573 in a disc of bounded radius in the complex plane. A numerical study has confirmed  
574 these results.

575 A point that has not been discussed in the paper is the quality of the threshold  
576 estimates. In practice it appears that the theoretical threshold are rather far from the  
577 “real” thresholds found numerically, as shown in Fig. 7. For instance, instabilities  
578 are found numerically to develop for  $U > U_c^{num}$  and the theoretical threshold  $U_c$ ,  
579 obtained in closed form, is not a good approximation of  $U_c^{num}$  (see Fig. 6 (a) where  
580  $U_c = 0.18$  and  $U_c^{num} = 0.4$ ). We do not know how to improve our estimates since we  
581 have already used Poincaré’s inequalities with adjustable parameters (see Eq. (16)  
582 and (17)) to be the most accurate as we could. However, our results are useful since  
583 they define a stability area which, although it could be larger, gives a security area  
584 to avoid instabilities, which is what we wish the most in practice.

## 585 Appendix A. Modes of the duct.

586 **A.1. Characterization of the modes.** The acoustic propagation in the half  
587 duct without plate, in presence of a uniform flow, can be completely described by  
588 computing the modes of the duct. These modes are the solutions with separated

589 variables  $(\varphi(x, y) = e^{i\beta x}\theta(y))$  of:

$$590 \quad \left\{ \begin{array}{l} \left( \frac{\partial^2}{\partial x^2} + \frac{1}{\alpha^2} \frac{\partial^2}{\partial y^2} \right) \varphi = \frac{1}{c^2} \left( U \frac{\partial}{\partial x} - i\omega \right)^2 \varphi \quad \text{in } \Omega, \\ \frac{\partial \varphi}{\partial y}(x, 1) = 0 \quad \text{on } \Sigma, \\ \varphi(x, 0) = 0 \quad \text{for } x \in \mathbb{R}. \end{array} \right.$$

591 Introducing the transverse functions

$$592 \quad \theta_n(y) = \sqrt{2} \sin \left[ \pi \left( n - \frac{1}{2} \right) y \right], n \geq 1,$$

593 forming a basis of  $\{\theta(y) \in H^1(0, 1)/\theta(0) = 0\}$ , the modes read

$$594 \quad \varphi_n^\pm(x, y) = e^{i\beta_n^\pm x} \theta_n(y),$$

595 with

$$596 \quad \beta_n^\pm = \frac{-kM \pm \gamma_n}{1 - M^2} \quad \text{where } k = \frac{\omega}{c},$$

$$597 \quad (26) \quad \gamma_n = \sqrt{k^2 - (1 - M^2)\zeta_n^2},$$

$$598 \quad \zeta_n = \frac{\pi}{\alpha} \left( n - \frac{1}{2} \right), n \geq 1.$$

599 To define  $\gamma_n$ , the chosen definition of the complex square root is:  $\sqrt{z} = \sqrt{r}e^{i\theta/2}$  for  
600  $z = re^{i\theta}$ ,  $\theta \in [0, 2\pi[$ . This definition of the complex square root leads to  $\Im m(\gamma_n) \geq 0$   
601 for any  $\omega \in \mathbb{C}$ .

602 The characteristics of the modes depend on the nature of  $\omega$ :  $\omega \in \mathbb{R}$  or  $\omega \in \mathbb{C} \setminus \mathbb{R}$ .

603 • For real values of  $\omega \in \mathbb{R}$ , we get

$$604 \quad \gamma_n = \sqrt{k^2 - (1 - M^2)\zeta_n^2} \quad \text{for } n - \frac{1}{2} < \frac{k\alpha}{\pi\sqrt{1 - M^2}},$$

$$605 \quad \gamma_n = i\sqrt{(1 - M^2)\zeta_n^2 - k^2} \quad \text{for } n - \frac{1}{2} > \frac{k\alpha}{\pi\sqrt{1 - M^2}}.$$

606 Therefore a finite number of propagative modes ( $\beta_n^\pm \in \mathbb{R}$ ) exist and an infinite number  
607 of evanescent modes ( $\beta_n^\pm \in i\mathbb{R}$  with  $\pm \Im m(\beta_n^\pm) > 0$ ) exist. The + modes “propagate”  
608 downstream: when they are propagative, they correspond to a positive group velocity  
609 and when they are evanescent, they decrease when  $x \rightarrow \infty$ . Symmetrically, the –  
610 modes propagate upstream.

611 For low frequencies,  $k < k_c \equiv \pi\sqrt{1 - M^2}/(2\alpha)$ , the so-called cut-off wave number  
612 of the half-guide, all the modes are evanescent and this is a good framework when  
613 looking for trapped modes.

614 • For complex values of  $\omega$ ,  $\omega \in \mathbb{C} \setminus \mathbb{R}$ , all the modes are evanescent since it is  
615 straightforward to verify that  $\pm \Im m(\beta_n^\pm) > 0$  and the + modes are downstream modes  
616 whereas the – modes are upstream modes.

617 **A.2. Transparent boundary conditions.** Let us point out that the duct  
618 modes are useful since every fluid vibration propagating outside the duct part in-  
619 cluding the plate can be decomposed on these modes. More precisely, if we introduce  
620 the vertical boundaries

$$621 \quad \Sigma_R^\pm = \{(x, y), x = \pm R, y \in ]0, 1[ \},$$

622 and remembering that the plate is of length 1, we have the

623 LEMMA 13. For any  $R > 1$ , for any  $\pm x \geq R$ , a solution of (2) belonging to  
624  $H^1(\Omega)$  can be written:

$$625 \quad (27) \quad \varphi(x, y) = \sum_{n \geq 1} a_n^\pm e^{i\beta_n^\pm(x \mp R)} \theta_n(y),$$

626 with

$$627 \quad a_n^\pm = (\varphi, \theta_n)_{\Sigma_R^\pm} \equiv \int_0^1 \varphi(\pm R, y) \theta_n(y) dy.$$

628 *Proof.* For any  $x \notin [0, 1]$ , which corresponds to be located in the duct outside the  
629 plate, the velocity potential can be decomposed on the duct modes:

$$630 \quad \varphi(x, y) = \sum_{n \geq 1} a_n^\pm e^{i\beta_n^\pm(x \mp R)} \theta_n(y).$$

631 The coefficient  $a_n^\pm$  are deduced, using the orthogonality of the transverse functions

$$632 \quad (\theta_n, \theta_m)_{\Sigma_R^\pm} = \delta_{mn} \quad \text{for any } n, m \geq 1. \quad \square$$

633 Using (27), we can define (exact) transparent boundary conditions thanks to DtN  
634 (Dirichlet to Neumann) operators  $T^\pm$ : for any  $R > 1$ ,

$$635 \quad (28) \quad \begin{aligned} \frac{\partial \varphi}{\partial x}(x = \pm R, y) &= T^\pm \varphi(x = \pm R, y) \quad \text{with} \\ T^\pm : \quad H^{1/2}(\Sigma_R^\pm) &\rightarrow H^{-1/2}(\Sigma_R^\pm), \\ \varphi(\pm R, y) &\rightarrow \pm i\beta_n^\pm (\varphi, \theta_n)_{\Sigma_R^\pm} \theta_n(y). \end{aligned}$$

### 636 Appendix B. Proof of lemma 3 for the continuous resonance problem.

637

638 To prove that if  $\omega$  is a resonance frequency, then  $\bar{\omega}$  is also a resonance frequency,  
639 we proceed in different steps:

- 640 • for the resonance problem (2) set in an unbounded domain, we define an
- 641 equivalent formulation (29) set in a bounded domain,
- 642 • in the bounded domain, thanks to a compacity property we prove that the
- 643 resonance problem is of Fredholm type,
- 644 • we conclude using the fact that  $A^*(\omega) = A(\bar{\omega})$  and the property  $\text{Ker } A^*(\omega) =$   
645  $(\text{Ran } A(\omega))^\perp$ .

646 **B.1. Resonance problem set in a bounded domain.** Thanks to the defini-  
647 tion of the radiation conditions at finite distance (28), we can introduce two equivalent  
648 ways to define the trapped modes: in an unbounded domain or in a domain bounded  
649 by radiation conditions. The unbounded problem has been defined in (2). The prob-  
650 lem can also be set in a bounded domain, using the DtN operator (28) to write  
651 transparent boundary conditions on the boundaries of the domain. In this aim we  
652 note for any  $R > 1$  (to include the whole plate)

$$653 \quad \Omega_R = \{(x, y) \in \Omega, |x| < R\} \quad \text{and} \quad \Gamma_R^\pm = \{(x, y) \in \Gamma^\pm, |x| < R\},$$

654 the bounded domains and we introduce the new solution space

$$655 \quad V_R = \{\varphi \in H^1(\Omega_R), \varphi = 0 \text{ on } \Gamma_R^\pm\}.$$

656 Then the problem of finding trapped mode takes the form: Find  $(\varphi, u) \in V_R \times W$   
657 such that

$$658 \quad (29) \quad \left\{ \begin{array}{l} \left( \frac{\partial^2}{\partial x^2} + \frac{1}{\alpha^2} \frac{\partial^2}{\partial y^2} \right) \varphi = \frac{1}{c^2} \left( U \frac{\partial}{\partial x} - i\omega \right)^2 \varphi \quad \text{in } \Omega_R, \\ \left( \frac{d^4}{dx^4} - \omega^2 \right) u = 2\mu \left( U \frac{\partial}{\partial x} - i\omega \right) \varphi(x, 0) \quad \text{on } \Gamma, \\ \frac{1}{\alpha} \frac{\partial \varphi}{\partial y}(x, 0) = \left( U \frac{\partial}{\partial x} - i\omega \right) u \quad \text{on } \Gamma, \\ \frac{\partial \varphi}{\partial x} = \pm i\beta_n^\pm (\varphi, \theta_n)_{\Sigma_R^\pm} \theta_n(y) \quad \text{on } \Sigma_R^\pm, \\ \frac{\partial \varphi}{\partial y}(x, 1) = 0 \quad \text{on } \Sigma_R, \\ u(0) = 0 = u'(0) \quad \text{and} \quad u''(1) = 0 = u^{(3)}(1). \end{array} \right.$$

659 To justify this problem we will prove that (29) is equivalent to (2).

660 **B.2. Equivalence between the bounded and unbounded problems.** Prob-  
661 lems (2) and (29) are equivalent. One implication is easy: (2) implies (29) since (29)  
662 is obtained by restricting the solution of (2) to  $\Omega_R$ . The reverse is less obvious but  
663 is true since a solution of (29) can be extended in a solution of (2), using (27). The  
664 only difficulty is to check that the extended solution is in  $H^1(\Omega)$ . When  $\omega \in \mathbb{C} \setminus \mathbb{R}$ ,  
665 the fact that all the duct modes are evanescent insures that the extension belongs to  
666  $H^1(\Omega)$ . When  $\omega \in \mathbb{R}$ , we have first to prove that the solution of (29) does not excite  
667 the propagating modes. In this aim, we write the variational form of (29):

668 (30) Find  $(\varphi, u) \in V_R \times W$  such that  $a_R[\omega; (\varphi, u), (\psi, v)] = 0$  for all  $(\psi, v) \in V_R \times W$ ,

669 with

$$670 \quad a_R[\omega; (\varphi, u), (\psi, v)] = a_{fluid}[\omega; (\varphi, u), (\psi, v)] + a_{plate}[\omega; (\varphi, u), (\psi, v)],$$

671 and

$$672 \quad a_{fluid}[\omega; (\varphi, u), (\psi, v)] =$$

$$673 \quad \int_{\Omega_R} \left[ (1 - M^2) \frac{\partial \varphi}{\partial x} \overline{\frac{\partial \psi}{\partial x}} + \frac{1}{\alpha^2} \frac{\partial \varphi}{\partial y} \overline{\frac{\partial \psi}{\partial y}} - i \frac{\omega}{c} M \left( \frac{\partial \varphi}{\partial x} \overline{\psi} - \varphi \overline{\frac{\partial \psi}{\partial x}} \right) - \frac{\omega^2}{c^2} \varphi \overline{\psi} \right],$$

$$674$$

$$675 \quad + \frac{1}{\alpha} \int_{\Gamma} \overline{\psi} \left( U \frac{\partial u}{\partial x} - i\omega u \right) - i \sum_{n \geq 1} \gamma_n(\omega) (\varphi, \theta_n)_{\Sigma_R^\pm} (\theta_n, \psi)_{\Sigma_R^\pm},$$

676 with  $\gamma_n$  defined in (26) and

$$677 \quad a_{plate}[\omega; (\varphi, u), (\psi, v)] = \frac{1}{2\mu\alpha} \int_{\Gamma} \left( \frac{d^2 u}{dx^2} \frac{d^2 \overline{v}}{dx^2} - \omega^2 u \overline{v} \right) + \frac{1}{\alpha} \int_{\Gamma} \varphi \left( U \frac{\partial \overline{v}}{\partial x} + i\omega \overline{v} \right).$$

678 Then, choosing  $(\psi, v) = (\varphi, u)$ , we take the imaginary part of (30)

$$679 \quad \Im m(a_R[\omega; (\varphi, u), (\varphi, u)]) = 0, \quad \text{which leads to } \sum_{n \geq 1} \Re e(\gamma_n) |(\varphi, \theta_n)_{\Sigma_R^\pm}|^2 = 0.$$

680 Since  $\Re e(\gamma_n) = 0$  for the evanescent modes for  $\omega \in \mathbb{R}$ , it leads to  $(\varphi, \theta_n)_{\Sigma_R^\pm} = 0$  for  
681 all the propagating modes. Therefore the extended solution (27) is purely evanescent  
682 and belongs to  $H^1(\Omega)$  and we have proved that (29) implies (2).

683 **B.3. Fredholm alternative.** Thanks to the Riesz theorem we can introduce  
684 the operator  $A(\omega)$  such that for all  $(\varphi, u)$  in  $V_R \times W$  and all  $(\psi, v)$  in  $V_R \times W$ ,

$$685 \quad (A(\omega)(\varphi, u), (\psi, v))_{V_R \times W} = a_R[\omega; (\varphi, u), (\psi, v)],$$

686 where we use the scalar product on  $V_R \times W$ :

$$687 \quad ((\varphi, u), (\psi, v))_{V_R \times W} = \\
688 \quad \int_{\Omega_R} \left[ \frac{\partial \varphi}{\partial x} \frac{\partial \bar{\psi}}{\partial x} + \frac{\partial \varphi}{\partial y} \frac{\partial \bar{\psi}}{\partial y} + \varphi \bar{\psi} \right] dx dy + \int_{\Gamma} \left( \frac{d^2 u}{dx^2} \frac{d^2 \bar{v}}{dx^2} + \frac{du}{dx} \frac{d\bar{v}}{dx} + u \bar{v} \right) dx.$$

690 Then the problem (30) can be written in an operator form: find  $\omega \in \mathbb{C}$  such that  
691 exists  $(\varphi, u)$  in  $V_R \times W$  satisfying  $A(\omega)(\varphi, u) = 0$ . The operator  $A$  is decomposed as  
692  $A = B + C$  where

$$693 \quad \bullet (B(\omega)(\varphi, u), (\psi, v))_{V_R \times W} = \int_{\Omega_R} \left[ (1 - M^2) \frac{\partial \varphi}{\partial x} \frac{\partial \bar{\psi}}{\partial x} + \frac{1}{\alpha^2} \frac{\partial \varphi}{\partial y} \frac{\partial \bar{\psi}}{\partial y} + \varphi \bar{\psi} \right], \\
694 \quad \frac{1}{2\mu\alpha} \int_{\Gamma} \left( \frac{d^2 u}{dx^2} \frac{d^2 \bar{v}}{dx^2} + u \bar{v} \right) - i \sum_{n \geq 1} \gamma_n(\omega) (\varphi, \theta_n)_{\Sigma_R^\pm} (\theta_n, \psi)_{\Sigma_R^\pm}, \\
695 \quad \bullet (C(\omega)(\varphi, u), (\psi, v))_{V_R \times W} = \int_{\Omega_R} \left[ -i \frac{\omega}{c} M \left( \frac{\partial \varphi}{\partial x} \bar{\psi} - \varphi \frac{\partial \bar{\psi}}{\partial x} \right) - \left( 1 + \frac{\omega^2}{c^2} \right) \varphi \bar{\psi} \right], \\
696 \quad + \frac{1}{\alpha} \int_{\Gamma} \bar{\psi} \left( U \frac{\partial u}{\partial x} - i\omega u \right) - \frac{1 + \omega^2}{2\mu\alpha} \int_{\Gamma} u \bar{v} + \frac{1}{\alpha} \int_{\Gamma} \varphi \left( U \frac{\partial \bar{v}}{\partial x} + i\omega \bar{v} \right).$$

699 The sesquilinear form  $b_R[\omega; (\varphi, u), (\psi, v)] = (B(\omega)(\varphi, u), (\psi, v))_{V_R \times W}$  is coercive on  
700  $V_R \times W$  which proves that  $B(\omega)$  is an isomorphism of  $V_R \times W$ . Indeed

$$701 \quad \exists C_R > 0, \forall (\varphi, u) \in V_R \times W, \Re e (b_R[\omega; (\varphi, u), (\varphi, u)]) \geq C_R \|(\varphi, u)\|_{V_R \times W}^2.$$

702 The key point is that

$$703 \quad \Re e \left( -i \sum_{n \geq 1} \gamma_n(\omega) (\varphi, \theta_n)_{\Sigma_R^\pm} (\theta_n, \varphi)_{\Sigma_R^\pm} \right) = \sum_{n \geq 1} \Im m(\gamma_n) |(\varphi, \theta_n)_{\Sigma_R^\pm}|^2 \geq 0,$$

704 since  $\Im m(\gamma_n(\omega)) \geq 0$ . It is also straightforward to prove that  $C(\omega)$  is a compact  
705 operator on  $V_R \times W$ , the key point being the Rellich theorem which applies since  $\Omega_R$   
706 is bounded.

707 The resonance problem  $(B + C)(\varphi, u) = 0$  can be written  $(I + B^{-1}C)(\varphi, u) = 0$   
708 because  $B$  is an isomorphism. And finally since  $B^{-1}C$  is a compact operator, the  
709 Fredholm alternative holds for this equation.

710 **B.4. Characteristics of the eigenvalues.** The Fredholm property obtained  
711 in the previous paragraph implies in particular, for the operator  $S = I + B^{-1}C$  but  
712 also for the operator  $A \equiv BS = B + C$  (since  $B$  is an isomorphism), that

- 713  $\bullet \text{Ker } A(\omega) = \{0\} \Leftrightarrow \text{Ran } A(\omega) = V_R \times W,$
- 714  $\bullet \text{Ker } A^*(\omega) = (\text{Ran } A(\omega))^\perp$  where  $A^*(\omega)$  is the adjoint of  $A(\omega)$ .
- 715 Moreover it is easy to prove  $A^*(\omega) = A(\bar{\omega})$ . This is in particular due to  $\gamma_n(\bar{\omega}) =$   
716  $-\gamma_n(\omega)$ .

717 Therefore, combining together the previous results, we get  $\text{Ker } A(\omega) = \{0\} \Leftrightarrow$   
 718  $\text{Ran } A(\omega) = V_R \times W \Leftrightarrow \text{Ker } A^*(\omega) = \{0\}$ . In other words  $\text{Ker } A(\omega) \neq \{0\} \Leftrightarrow$   
 719  $\text{Ker } A(\bar{\omega}) \neq \{0\}$  and thus if  $\omega$  is a resonance frequency, then  $\bar{\omega}$  is also a resonance  
 720 frequency.

721 Finally, we have proved that if  $\omega$  is an eigenvalue then  $\pm\bar{\omega}$  are also eigenvalues.  
 722 But then, since  $\bar{\omega}$  is an eigenvalue,  $\pm\omega$  are also eigenvalues which ends the proof of  
 723 lemma 3.

### 724 **Appendix C. Numerical method.**

725 We start from the formulation of the trapped modes problem set in a bounded  
 726 domain (30). Noting  $(w_j)_{j=1 \dots N_{\text{dof}}}$  the finite element basis (P1 elements) with  $N_{\text{dof}}$   
 727 the number of degrees of freedom, the velocity potential is sought under the form

$$728 \quad \varphi = \sum_{j=1}^{N_{\text{dof}}} \varphi_j w_j(x, y),$$

729 where the nodal values  $\varphi_j$  are unknowns. Also using the modal basis of the plate  
 730  $(\xi_m)_{m \geq 1}$  Eq. (33), the displacement of the plate is sought under the form

$$731 \quad u = \sum_{n=1}^{N_{\text{pl}}} u_n \xi_n(x),$$

732 where the modal components  $u_n$  are unknowns and  $N_{\text{pl}}$  is the number of plate modes  
 733 taken into account. Then, developing

$$734 \quad a_{\text{fluid}} \left[ \omega; \left( \sum_{j=1}^{N_{\text{dof}}} \varphi_j w_j, \sum_{n=1}^{N_{\text{pl}}} u_n \xi_n \right), (w_i, \xi_m) \right] = 0,$$

735 and

$$736 \quad a_{\text{plate}} \left[ \omega; \left( \sum_{j=1}^{N_{\text{dof}}} \varphi_j w_j, \sum_{j=1}^{N_{\text{pl}}} u_n \xi_n \right), (w_i, \xi_m) \right] = 0,$$

737 for all  $i = 1$  to  $N_{\text{dof}}$  and all  $m = 1$  to  $N_{\text{pl}}$ , we are lead to define the matrices

$$738 \quad D_{ij} = (1 - M^2) \left( \frac{\partial w_j}{\partial x}, \frac{\partial w_i}{\partial x} \right)_{\Omega_R} + \frac{1}{\alpha^2} \left( \frac{\partial w_j}{\partial y}, \frac{\partial w_i}{\partial y} \right)_{\Omega_R},$$

$$739 \quad E_{ij} = \frac{M}{c} \left[ \left( w_j, \frac{\partial w_i}{\partial x} \right)_{\Omega_R} - \left( \frac{\partial w_j}{\partial x}, w_i \right)_{\Omega_R} \right],$$

$$740 \quad M_{ij}(\omega) = -i \sum_{p=1}^{N_{\text{DfN}}} \gamma_p(\omega) \zeta_p(w_j, \theta_p)_{\Sigma_R^\pm} (\theta_p, w_i)_{\Sigma_R^\pm},$$

741

742 and

$$743 \quad F_{ij} = \left( -\frac{1}{c^2} \right) (w_j, w_i)_{\Omega_R}, \quad G_{in} = \frac{U}{\alpha} \left( \frac{d\xi_n}{dx}, w_i \right)_{\Gamma}, \quad H_{in} = \left( -\frac{1}{\alpha} \right) (\xi_n, w_i)_{\Gamma},$$

744

$$745 \quad I_{mn} = \frac{1}{2\mu\alpha} \left( \frac{d^2 \xi_n}{dx^2}, \frac{d^2 \xi_m}{dx^2} \right)_{\Gamma}, \quad J_{mn} = \left( -\frac{1}{2\mu\alpha} \right) (\xi_n, \xi_m)_{\Gamma}.$$

746  $N_{\text{DtN}}$  is the number of term taken to describe the DtN operators. Thanks to the  
747 defined matrices, the discretized resonance problem is

$$748 \quad (31) \quad \begin{pmatrix} D + i\omega E + \omega^2 F + M(\omega) & G + i\omega H \\ G^T - i\omega H^T & I + \omega^2 J \end{pmatrix} \begin{pmatrix} \Phi \\ U \end{pmatrix} = 0,$$

749 where we have introduced the vectors of unknowns

$$750 \quad \Phi = (\varphi_1, \dots, \varphi_{N_{\text{dof}}})^T \quad \text{and} \quad U = (\xi_1, \dots, \xi_{N_{\text{pl}}})^T.$$

751 This is a non-linear eigenvalue problem because of the matrix  $M(\omega)$  which includes  
752  $\gamma_n(\omega)$  defined in Eq. (26) as a square root of  $\omega$ . To simplify the study, we have ap-  
753 proximated the matrix  $M$  to get a quadratic eigenvalues problem. Several approaches  
754 are possible and we have checked that they give very similar results. The simplest  
755 possibility is to replace the transparent boundary conditions (28) by homogeneous  
756 Neumann or Dirichlet boundary conditions:

$$757 \quad \frac{\partial \varphi}{\partial x} = 0 \quad \text{or} \quad \varphi = 0 \quad \text{on} \quad \Sigma_R^\pm.$$

758 Since the velocity potential decreases exponentially away from the plate, these ap-  
759 proximations are very good if  $\Sigma_R^\pm$  is far enough from the plate. In both cases, we  
760 get that the matrix  $M = 0$ . The Dirichlet case requires an extra element: the finite  
761 element basis  $(w_j)_{j=1 \dots N_{\text{dof}}}$  must satisfy the Dirichlet condition.

762 We have chosen another approach which consists in replacing  $\gamma_n = \sqrt{k^2 - (1 - M^2)\zeta_n^2}$   
763 by the approximation  $\tilde{\gamma}_n = i\sqrt{1 - M^2}\zeta_n$ . This is the natural approximation when  
764  $n \rightarrow \infty$ . It leads to the approximation  $\tilde{M}$  of the matrix  $M$ , independent of the  
765 frequency and defined by

$$766 \quad \tilde{M}_{ij} = \sqrt{1 - M^2} \sum_{p=1}^{N_{\text{DtN}}} \zeta_p (w_j, \theta_p)_{\Sigma_R^\pm} (\theta_p, w_i)_{\Sigma_R^\pm}.$$

767 We have chosen this approximation because it is close from the true radiation con-  
768 ditions and it becomes exact for large  $p$  values. Moreover it is easy to implement  
769 numerically.

770 To write the quadratic eigenvalue problem as a classical eigenvalue problem, we  
771 introduce the matrices:

$$772 \quad A = \begin{pmatrix} D + M & G \\ G^T & 0 \end{pmatrix}, \quad B = \begin{pmatrix} E & H \\ -H^T & 0 \end{pmatrix}, \quad C = \begin{pmatrix} F & 0 \\ 0 & J \end{pmatrix},$$

773 where  $A$ ,  $B$  and  $C$  are real matrices with  $A^T = A$ ,  $B^T = -B$  (since  $E^T = -E$ ) and  
774  $C^T = C$ . Then (31) reads

$$775 \quad (A + i\omega B + \omega^2 C)X = 0,$$

776 where  $X$  is the vector  $(\Phi, U)^T$ .

777 The Finite Element matrices are built using a Finite Elements code [33] and the  
778 eigenvalues are determined using the Matlab software. For a domain of size  $2 \times 1$ , we  
779 use an unstructured triangular mesh, we introduce P1 finite elements and in practice  
780 we take  $N_{\text{dof}} = 2309$ ,  $N_{\text{pl}} = 6$  and  $N_{\text{DtN}} = 10$ . We have checked that taking larger  
781 values doesn't change significantly the results.

782 **Appendix D. Simplification of the theoretical estimates.**



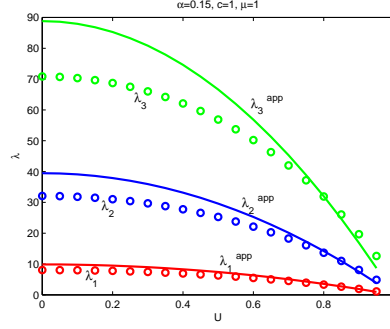


FIG. 8. Three first eigenvalues  $\lambda_n$  of problem (32) versus  $U$  for  $\alpha = 0.15$  and  $c = 1$ . Circles: exact values, Solid lines: approximations  $\lambda_n^{\text{app}}$

783 Here we show that  $\hat{\sigma}$  defined in (11) can be approximated by (20) that we recall

$$784 \quad \sigma = \min [(c^2 - U^2)\pi^2, \alpha_1^4].$$

785 Indeed the values of  $\lambda_1$  and  $\alpha_1^4$ , introduced in (8) and (10), can be obtained in  
786 closed form, as explained now.

787 • Approximation of  $\lambda_1$ :

788 Since

$$789 \quad \lambda_1 = \inf_{\varphi \in V} R(\varphi),$$

790 with  $R$  defined in (9), using the test field  $\varphi_0 \in V$  defined by

$$791 \quad \begin{cases} \varphi_0(x, y) = \sin(\pi x) & \text{for } x \in ]0, 1[, \\ \varphi_0(x, y) = 0 & \text{for } x \notin ]0, 1[, \end{cases}$$

792 we find the upper bound

$$793 \quad \lambda_1 \leq R(\varphi_0) = (c^2 - U^2)\pi^2.$$

794 We have determined numerically that this upper bound  $(c^2 - U^2)\pi^2$  is in fact a good  
795 approximation of  $\lambda_1$ . To do so and to find the numerical value of  $\lambda_1$ , we notice that  
796  $\lambda_1$  is also the first eigenvalues of the problem: find  $\varphi \in V$  and  $\lambda \in \mathbb{R}$  such that

$$797 \quad (32) \quad \begin{cases} -(c^2 - U^2) \frac{\partial^2 \varphi}{\partial x^2} - \frac{c^2}{\alpha^2} \frac{\partial^2 \varphi}{\partial y^2} = \lambda \varphi & \text{in } \Omega, \\ \frac{1}{\alpha} \frac{\partial \varphi}{\partial y}(x, 0) = 0 & \text{on } \Gamma, \\ \frac{\partial \varphi}{\partial y}(x, 1) = 0 & \text{on } \Sigma. \end{cases}$$

798 Indeed the Min-Max principle indicates that  $\lambda_1$  defined by (8) thanks to the Rayleigh  
799 quotient (9) is the first eigenvalue if  $\lambda_1 < (\pi c / 2\alpha)^2$  (below the essential spectrum).

800 For  $\alpha = 0.15$  and  $c = 1$ , in Fig. 8 are plotted with solid lines the three first  
801 eigenvalues  $\lambda_n$ ,  $n = 1, 2$  and  $3$ , of problem (32) versus  $U$  below the essential spectrum  
802  $((\pi c / 2\alpha)^2 \simeq 110)$ , obtained numerically thanks to a Finite Element method. The  
803 circles represent the values  $\lambda_n^{\text{app}} \equiv n^2 \pi^2 (c^2 - U^2)$  versus  $U$  for  $n = 1, 2$  and  $3$ . We  
804 see that for  $n = 1$ ,  $\lambda_1^{\text{app}} = \pi^2 (c^2 - U^2)$  approximates very accurately  $\lambda_1$ . On the

805 contrary, the approximations  $\lambda_n^{\text{app}}$  of  $\lambda_n$  for  $n = 2$  and  $3$  are not satisfactory (they  
806 become better approximations when  $\alpha$  is decreased, result not reported here).

807 • Approximation of  $\alpha_1$ :

808 To determine  $\alpha_1$ , we introduce the following eigenvalue problem: find  $u \in W$  and  
809  $\lambda^{\text{plate}} \in \mathbb{R}$  such that

$$810 \quad \frac{d^4 u}{dx^4} = \lambda^{\text{plate}} u \quad \text{for } x \in ]0, 1[,$$

$$811 \quad u''(1) = 0 = u^{(3)}(1).$$

812 This is the equation of the plate in vacuum and the eigenvalues  $\lambda_n^{\text{plate}}$  are equal to the  
813 square of the eigenfrequencies  $\omega_n^{\text{plate}}$  of the plate. A simple explicit calculation shows  
814 that  $\lambda_n^{\text{plate}} = \alpha_n^4$  with  $\alpha_n$  satisfying [1, 9]

$$815 \quad \cos \alpha_n \cosh \alpha_n = -1.$$

816 In particular,  $\alpha_1 = 1.88$ . The eigenmodes are

$$817 \quad (33) \quad \xi_n(x) = A_n [\sinh(\alpha_n x) - \sin(\alpha_n x)] + B_n [\cosh(\alpha_n x) - \cos(\alpha_n x)],$$

818 where

$$819 \quad B_n = -A_n \frac{\sinh(\alpha_n) + \sin(\alpha_n)}{\cosh(\alpha_n) + \cos(\alpha_n)},$$

820 and  $A_n$  can be chosen such that  $\int_{\Gamma} |\xi_n|^2 = 1$ . Finally the Min-Max principle indicates

821 that  $\lambda_1^{\text{plate}}$  satisfies

$$822 \quad \lambda_1^{\text{plate}} = \inf_{u \in W} \frac{\int_{\Gamma} \left| \frac{d^2 u}{dx^2} \right|^2}{\int_{\Gamma} |u|^2},$$

823 in accordance with (10).

824

#### REFERENCES

- 825 [1] A.-S. Bonnet-Ben Dhia, and J.-F. Mercier, “Resonances of an elastic plate in a compressible  
826 confined fluid.”, The Quarterly Journal of Mechanics and Applied Mathematics 60(4),  
827 397-421 (2007)
- 828 [2] A.-S. Bonnet-Ben Dhia, and J.-F. Mercier, “Resonances of an elastic plate coupled with a com-  
829 pressible confined flow.”, The Quarterly Journal of Mechanics and Applied Mathematics  
830 62(2), 105-129 (2009)
- 831 [3] H. Dowell, C. Curtiss Jr., R. H. Scanlan, F. Sisto, “A Modern Course in Aeroelasticity”, Kluwer  
832 Academic Publishers (1989)
- 833 [4] Y.C. Fung, “An Introduction to the Theory of Aeroelasticity”, J. Wiley, New York (1955)
- 834 [5] C. Eloy, R. Lagrange, C. Souilliez and L. Schouveiler, “Aeroelastic instability of cantilevered  
835 flexible plates in uniform flow”, J. Fluid Mech. 611, 97106 (2008)
- 836 [6] Y. Watanabe, S. Suzuki, M. Sugihara and Y. Sueoka, “An Experimental Study of Paper Flut-  
837 ter”, Journal of Fluids and Structures 16(4), 529542 (2002)
- 838 [7] Y. Watanabe, K. Isogai and S. Suzuki and M. Sugihara, “A Theoretical Study of Paper Flutter”,  
839 Journal of Fluids and Structures 16(4) 543560 (2002)
- 840 [8] T. S. Balint and A. D. Lucey, “Instability of a cantilevered flexible plate in viscous channel  
841 flow”, Journal of Fluids and Structures 20, 893912 (2005)
- 842 [9] C. Q. Guo and M. P. Paidoussis, “Stability of rectangular plates with free side-edges in two-  
843 dimensional inviscid channel flow.”, Journal of Applied Mechanics 67(1) 171-176 (2000)
- 844 [10] D. V. Evans, M. Levitin, and D. Vassiliev, “Existence theorems for trapped modes.”, Journal  
845 of Fluid Mechanics 261, 21-31 (1994)

- 846 [11] E. B. Davies, and L. Parnowski, “Trapped modes in acoustic waveguides.”, The Quarterly  
847 Journal of Mechanics and Applied Mathematics 51(3), 477-492 (1998)
- 848 [12] N. S. A. Khallaf, L. Parnowski, and D. Vassiliev, “Trapped modes in a waveguide with a long  
849 obstacle.”, Journal of Fluid Mechanics 403, 251-261 (2000)
- 850 [13] E. J. Brambley, and N. Peake, “Stability and acoustic scattering in a cylindrical thin shell  
851 containing compressible mean flow.”, Journal of Fluid Mechanics 602, 403-426 (2008)
- 852 [14] M. Vullierme-Ledard, “Asymptotic study of the vibration problem for an elastic body deeply  
853 immersed in an incompressible fluid”, Math. Model. Numer. Anal. 19, 145-170 (1985)
- 854 [15] E. Sanchez-Palencia, “Nonhomogeneous media and vibration theory”, Springer-Verlag, Berlin  
855 (1980)
- 856 [16] R. Ohayon and E. Sanchez-Palencia, “On the vibration problem for an elastic body surrounded  
857 by a slightly compressible fluid”, RAIRO Anal. Numr. 17, 311-326 (1983)
- 858 [17] J. Sanchez-Hubert and E. Sanchez-Palencia, “Vibration and Coupling of Continuous Systems,  
859 Asymptotics Methods”, Springer-Verlag, Berlin (1989)
- 860 [18] C. Conca, A. Osses, and J. Planchard, “Asymptotic Analysis Relating Spectral Models in  
861 Fluid–Solid Vibrations”, SIAM journal on numerical analysis 35(3), 1020-1048 (1998)
- 862 [19] P. Destuynder and E. Gout-D’hénin, “Existence and uniqueness of a solution to an aeroacoustic  
863 model”, Chinese Ann. Math. Ser. B 23, 11-24 (2002)
- 864 [20] P. Destuynder and J. Vétillard, “Modelling and control of noise in a flexible flow duct.”, Com-  
865 puter Methods in Applied Mechanics and Engineering 197(19), 1801-1812 (2008)
- 866 [21] L. Cot, J-P. Raymond, and J. Vancostenoble, “Exact controllability of an aeroacoustic model  
867 with a Neumann and a Dirichlet boundary control”, SIAM Journal on Control and Opti-  
868 mization 48(3), 1489-1518 (2009)
- 869 [22] J. Vétillard and P. Destuynder, “A noise control problem arising in a flow duct”, SIAM Journal  
870 on Applied Mathematics 64(6), 1987-2017 (2004)
- 871 [23] D. V. Evans, C. M. Linton, and F. Ursell, “Trapped mode frequencies embedded in the con-  
872 tinuous spectrum.”, The Quarterly Journal of Mechanics and Applied Mathematics 46(2),  
873 253-274 (1993):
- 874 [24] M. D. Groves, “Examples of Embedded Eigenvalues for Problems in Acoustic Waveguides”,  
875 Mathematical Methods in the Applied Sciences 21(6), 479-488 (1998)
- 876 [25] Porter, R., and D. V. Evans, “Embedded RayleighBloch surface waves along periodic rectan-  
877 gular arrays.”, Wave motion 43(1), 29-50 (2005)
- 878 [26] L. J. Ayton, J. R. Gill and N. Peake, “The importance of the unsteady Kutta condition when  
879 modelling gustaerofoil interaction.”, Journal of Sound and Vibration, 378, 28-37 (2016).
- 880 [27] W. Koch, “Resonant Acoustic Frequencies of Flat Plate Cascades”, Journal of Sound and  
881 Vibration 88(2), 233-242 (1983)
- 882 [28] N.C. Ovensden, W. Eversman, S.W. Rienstra, “Cut-on cut-off transition in flow ducts: compar-  
883 ing multiple-scales and finite-element solutions”, Paper AIAA 2004-2945 of the 10th  
884 AIAA/CEAS Aeroacoustics Conference, Manchester, UK, 10-12 May 2004
- 885 [29] A. Aslanyan, L. Parnowski, and D. Vassiliev, “Complex resonances in acoustic waveguides.”,  
886 The Quarterly Journal of Mechanics and Applied Mathematics 53(3), 429-447 (2000)
- 887 [30] Y. Duan, et al., “Complex resonances and trapped modes in ducted domains.” Journal of Fluid  
888 Mechanics 571, 119-147 (2007)
- 889 [31] M. Lenoir, M. Vullierme-Ledard, and C. Hazard, “Variational formulations for the determina-  
890 tion of resonant states in scattering problems.”, SIAM journal on mathematical analysis  
891 23(3), 579-608 (1992)
- 892 [32] C. Hazard, and M. Lenoir, “Determination of scattering frequencies for an elastic floating  
893 body.”, SIAM journal on mathematical analysis 24(6), 1458-1514 (1993)
- 894 [33] XLiFE++, eXtended Library of Finite Elements in C++, [https://uma.ensta-  
895 paristech.fr/soft/XLiFE++/](https://uma.ensta-paristech.fr/soft/XLiFE++/)